

University of Windsor

## Scholarship at UWindsor

---

Major Papers

Theses, Dissertations, and Major Papers

---

June 2021

### Exergy Analysis of A Small-Scale Trigenerative Compressed Air Energy Storage System

RAGHUVVEERA SAI SARATH DITTAKAVI  
dittaka@uwindsor.ca

Follow this and additional works at: <https://scholar.uwindsor.ca/major-papers>



Part of the [Energy Systems Commons](#)

---

#### Recommended Citation

DITTAKAVI, RAGHUVVEERA SAI SARATH, "Exergy Analysis of A Small-Scale Trigenerative Compressed Air Energy Storage System" (2021). *Major Papers*. 180.  
<https://scholar.uwindsor.ca/major-papers/180>

This Major Research Paper is brought to you for free and open access by the Theses, Dissertations, and Major Papers at Scholarship at UWindsor. It has been accepted for inclusion in Major Papers by an authorized administrator of Scholarship at UWindsor. For more information, please contact [scholarship@uwindsor.ca](mailto:scholarship@uwindsor.ca).

**Exergy Analyses of a Small-Scale  
Trigenerative Compressed Air Energy Storage System**

By

**Raghuveera Sai Sarath Dittakavi**

A Major Research Paper  
Submitted to the Faculty of Graduate Studies  
through the Department of Mechanical, Automotive and Materials  
Engineering in Partial Fulfillment of the Requirements for  
the Degree of Master of Applied Science  
at the University of Windsor

Windsor, Ontario, Canada

2021

© 2021 Raghuveera Sai Sarath Dittakavi

**Exergy Analyses of a Small-Scale  
Trigenerative Compressed Air Energy Storage System**

By

**Raghuveera Sai Sarath Dittakavi**

APPROVED BY:

---

J. Johrendt

Department of Mechanical, Automotive and Materials Engineering

---

R. Carriveau, Co-Advisor

Department of Civil and Environmental Engineering

---

D. Ting, Co-Advisor

Department of Mechanical, Automotive and Materials Engineering

May 21, 2021

## **DECLARATION OF ORIGINALITY**

I hereby certify that I am the sole author of this major paper and that a part of this major paper has been submitted for publication.

I certify that, to the best of my knowledge, my major paper does not infringe upon anyone's copyright nor does it violate any proprietary rights, and that any ideas, techniques, quotations, or any other material from the work of other people included in my major paper, published or otherwise, are fully acknowledged in accordance with the standard referencing practices. Furthermore, to the extent that I have included copyrighted material that surpasses the bounds of fair dealing within the meaning of the Canada Copyright Act, I certify that I have obtained written permission from the copyright owner(s) to include such material(s) in my major paper and that I have included copies of such copyright clearances in my appendix.

I declare that this is a true copy of my major paper, including any final revisions, as approved by my major paper committee and the Graduate Studies office, and that this major paper has not been submitted for a higher degree to any other University or Institution.

## ABSTRACT

Trigenerative compressed air energy storage (T-CAES) capitalizes on the heat of the compression process, something that is often wasted in more conventional CAES approaches. A T-CAES system with a 4-kW compressor and 2-kW turbine is thermodynamically analyzed in this study. Exergy analyses performed on each component in the system identify specific areas for improvement. It is found that, under actual conditions, more than half of the total exergy destruction is caused by the accumulator and about a quarter of the destruction is caused by the pressure regulator and turbine. Further, the pressure regulator, accumulator and turbine offer 66%, 27% and 32% of individual component recoverable exergies, respectively. These recoveries can improve the overall exergy efficiency of the system by 35%.

## **DEDICATION**

I dedicate this work to my parents, Dr. D. Ramachandran, and D. Sabitha, and to my sister, D. Saranya.

## ACKNOWLEDGEMENTS

I thank the Almighty for guiding me in every step of this work. I also extend my sincere gratitude to Dr. David Ting and Dr. Rupp Carriveau for giving me this opportunity to work at this wonderful university. I am grateful for all their guidance during the course of my studies.

I am grateful to Dr. Mehdi Ebrahimi, who was always there whenever I had any questions regarding the analyses.

I am forever indebted to everyone in the Turbulence & Energy Laboratory for all their help. I am also thankful to the Department of Mechanical, Automotive and Materials Engineering for their financial support in the form of my Graduate Assistantship.

I would also like to express my thankfulness to my family for their unconditional support and their confidence in me during my studies. Finally, I cannot thank my friends enough for being with me, especially Mr. Akash Mathew and Mr. Kousthub Mantha, during the entire duration of my master's program.

## TABLE OF CONTENTS

DECLARATION OF ORIGINALITY .....	iii
ABSTRACT .....	iv
ACKNOWLEDGEMENTS .....	vi
LIST OF TABLES .....	ix
LIST OF FIGURES .....	xi
LIST OF ABBREVIATIONS/SYMBOLS .....	xii
1. CHAPTER 1 INTRODUCTION AND LITERATURE REVIEW .....	1
1.1 Introduction to CAES.....	1
1.2 Trigenerative CAES .....	3
1.3 Literature review .....	11
2. CHAPTER 2 THERMODYNAMIC LAWS.....	17
2.1 The First Law of Thermodynamics.....	17
2.2 Exergy .....	19
2.3 Conditions used in exergy analysis.....	21
3. CHAPTER 3 T-CAES SYSTEM SETUP AND ANALYSES .....	28
3.1 System description .....	28
3.2 Compressors.....	29
3.3 Heat exchangers .....	30
3.4 Storage Tanks.....	31
3.5 Turbine .....	33
3.6 Thermodynamic (Exergy) analyses .....	34
3.7 Analysis methodology.....	36
4. CHAPTER 4 RESULTS AND DISCUSSIONS .....	39
4.1 Results and Discussions.....	39
5. CHAPTER 5 CONCLUSIONS .....	50



REFERENCES/BIBLIOGRAPHY.....	52
VITA AUCTORIS .....	57

## LIST OF TABLES

Table 2.1 Table providing the parametric data for the compressor [36]. .....	19
Table 2.2 Input and output parameters of a heat exchanger under actual conditions.....	22
Table 2.3 Input and output parameters of a heat exchanger under unavoidable working conditions.....	23
Table 2.4 Exergy values of the heat exchanger under actual and unavoidable conditions. ....	25
Table 2.5 Input and output parameters of an accumulator under two state conditions. ....	26
Table 2.6 Input and output parameters of a turbine under two state conditions.....	27
Table 2.7 The results of relative exergy destruction. ....	27
Table 3.1 Parametric considerations.....	36
Table 3.2 Energy and exergy balance equations for the components of the system. ....	38
Table 4.1 Parameters at first condition calculated using Equations 12 - 21 .....	40
Table 4.2 Parameters at second condition calculated using Equations 12 - 21 .....	41
Table 4.3 Results of the exergy analyses of small-scale T-CAES under actual working conditions calculated using Equations 28 - 32 .....	42
Table 4.4 Results of the exergy analyses of small-scale T-CAES under unavoidable working conditions calculated using Equations 28 - 32 .	42
Table 4.5 Results of accumulator. ....	44

Table 4.6 Improvement priority order for the components. .... 49

## LIST OF FIGURES

Figure 1.1 Classification of CAES based on type of design. ....	2
Figure 1.2 Example of trigenerative compressed air energy storage system. ....	4
Figure 1.3 D-CAES system (a) schematic (b) T-S diagram.....	5
Figure 1.4 A-CAES system (a) schematic (b) T-S diagram.....	7
Figure 1.5 I-CAES (a) schematic (b)T-S diagram.....	9
Figure 1.6 A summary of literature review on CAES.....	12
Figure 2.1 Steady state energy flow for a compressor. ....	18
Figure 2.2 Exergy flow of steady-state heat transfer through a wall. .	20
Figure 2.3 Exergy Flow in Heat-Exchanger.....	25
Figure 3.1 Schematic of the T-CAES system under consideration.....	28
Figure 4.1 Figure illustrating the exergy efficiencies under two working conditions. ....	44
Figure 4.2 Figure illustrating the relative exergy under two working conditions.....	46
Figure 4.3 Exergy destruction ratio under actual conditions.....	48
Figure 4.4 Exergy destruction ratio under unavoidable condition .....	48
Figure 4.5 Overall exergy destruction of the system.....	49

## LIST OF ABBREVIATIONS/SYMBOLS

A-CAES	Adiabatic Compressed air energy storage
ACC	Accumulator
CAES	Compressed air energy storage system
CS	Compressor stage
$C_p$	Heat capacity ( $\text{kJ kg}^{-1} \text{ } ^\circ\text{C}^{-1}$ )
E	Exergy (kW)
h	Enthalpy ( $\text{J kg}^{-1}$ )
HEX	Heat exchanger
$\dot{m}$	Mass flowrate ( $\text{kg s}^{-1}$ )
$N_c$	Number of compression stages
$N_{\text{res}}$	Number of storage tanks
PR	Pressure regulator
Q	Heat (J)
$R_g$	Gas constant ( $\text{N}\cdot\text{m}\cdot\text{kmol}^{-1}\cdot\text{K}^{-1}$ )
T-CAES	Trigenerative Compressed Air Energy Storage System
TUR	Turbine
T	Temperature (K)
T	Time (s)
UN	Unavoidable
V	Volume ( $\text{m}^3$ )
W	Work (W)
Y	Molar fraction

## Greek

$\beta_c$	Compression ratio
$\beta_d$	Expansion ratio
$\gamma$	Polytropic coefficient
$\varepsilon$	Effectiveness
$\eta$	Efficiency
$\Omega$	Air leakage ( $\text{kg s}^{-1}$ )

## Subscripts

C	Cold
H	Hot
A	Working fluid (air)
Ch	Charging
C	compression
D	Destruction in k-th component
Dis	Discharging
E	Expansion
Eff	Efficiency
F	Fuel
h, tes	Hot thermal energy storage
In	Input
I	Stage number
K	Component number

l, tes	Cold thermal energy storage
M	Mechanical
Out	Output
P	Product
Th	thermodynamic
Tot	Total
W	Heat transfer medium

# CHAPTER 1

## INTRODUCTION AND LITERATURE REVIEW

Replacing conventional energy conversion systems which run on fossil fuels with renewable energies is an effective way to help mitigate economic and environmental concerns. The intermittent nature of many renewable energy resources and the energy supply-demand mismatch call for energy storage. There are several energy storage systems, such as pumped hydroelectric storage systems, compressed air energy storage systems, thermal energy storage, batteries, and super-capacitors, among others. Among these options, compressed air energy storage (CAES) has great potential due to its high reliability, low capital and maintenance costs and good part-load performance [1].

### *1.1 Introduction to CAES*

In CAES, the energy to be stored is used to compress ambient air into storage tanks. When the need arises, the compressed air is converted to electrical energy by expanders [1-3]. The process of compressing air generates heat, and how that heat is dealt with is the main criterion in the classification of CAES systems, as shown in [Figure 1.1](#). There are three main types of CAES systems: 1) Diabatic-CAES (D-CAES); 2) Adiabatic-CAES (A-CAES); and 3) Isothermal-CAES (I-CAES).



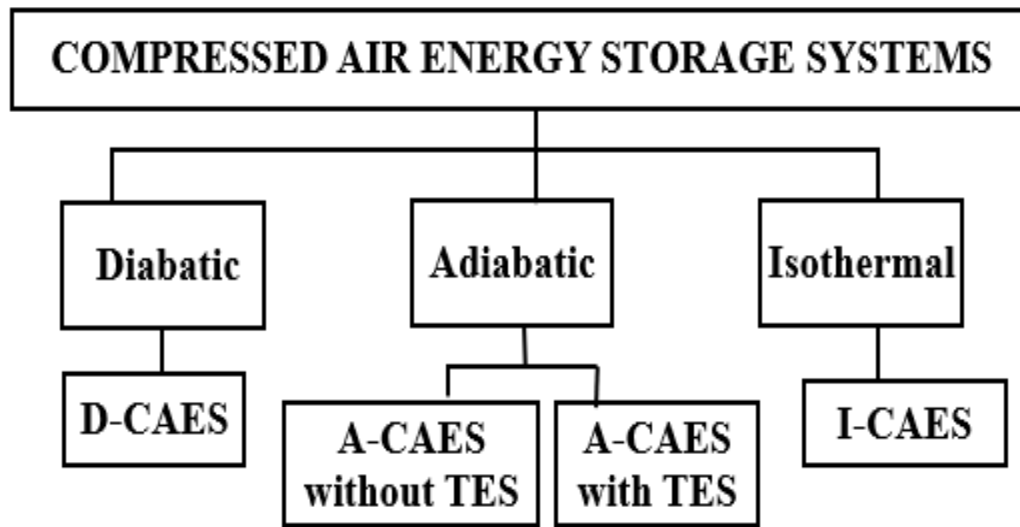


*Figure 1.1 Classification of CAES based on type of design.*

In D-CAES, the heat generated in the compression process is lost to the environment as waste heat [4-6]. Hence, an external heat source is needed to prevent condensation on the expander, which compromises system efficiency, which is around 40% to 53% [7]. This drawback has been rectified to an extent with the introduction of adiabatic compressed air energy storage systems (A-CAES). In A-CAES, the heat produced during the compression is collected and stored in a thermal energy storage (TES) system, and then used to preheat the air before expansion. Because of the recuperation and use of heat generated by compression, the system efficiency of A-CAES can be close to 65% [8]. This technology is significantly more advanced than D-CAES, and, thus, is also known as “advanced CAES.”

In the isothermal CAES (ICAES) process, the temperature is kept stable during the compression process. This lowers the power required to run the compressor below the amount required to run an adiabatic compressor with

the same pressure ratio. During the expansion, the associated heat is supplied constantly to ensure expansion at a constant temperature. Despite this, near-isothermal compression is yet to be used industrially [9]. The CAES approaches differ widely based on quantitative parameters like energy density, start-up time and cycle efficiency, as well as in more qualitative measures, like their states of commercialization.

### ***1.2 Trigenerative CAES***

The concept of trigenerative compressed air storage (T-CAES) [10,11] derives from the adiabatic classification. The trigenerative compressed air energy storage system (T-CAES) simplifies the actual of the A-CAES by removing the regenerative air re-heating. The heat eliminated during the compression phase is stored and, rather than being utilized to reheat the air at the turbine inlet, may be used to deliver a thermal energy demand [10]. As a corollary, air enters the expansion train at a low temperature, and chilling energy is obtained at the expander's outlet, without the need of an inverse cycle. Placing such a plant close to the energy user facilitates the effective utilization of all the energy streams.

The schematic of Trigenerative-CAES system is shown in [Figure 1.2](#). A CAES system generally consists of three phases. First, compression phase in which compressors and heat-exchangers are the key components. When mechanical or electrical energy is available, the compressor train begins pumping the air in the environment into high pressure reservoirs. In between each compression phase heat-exchangers are used to capture the heat generated and store them in the thermal energy storage tanks. Second, storage phase where the compressed air with high pressures is stored in the

storage tanks. Finally, the system ends with expansion phase where power is generated through expansion. Since thermal energy is stored and utilized on a daily basis, the heat storage does not pose any particular technological problems, as it may be simply achieved through a properly insulated tank. There is a significant increase in system efficiency to 68%, which is slightly higher than the A-CAES system's efficiency of 63% [8]. When mechanical energy is necessary from the T-CAES, the air stored in the high-pressure storage tanks is expanded through a reheated multistage turbine train, without usage of additional fuel. As for the compression, the optimal choice for the expansion technology depends on the expansion ratio and mass flow rate; it is commonly assumed that one could switch to a small centrifetal turbine whilst still having to use a volumetric compressor to obtain high efficiency.

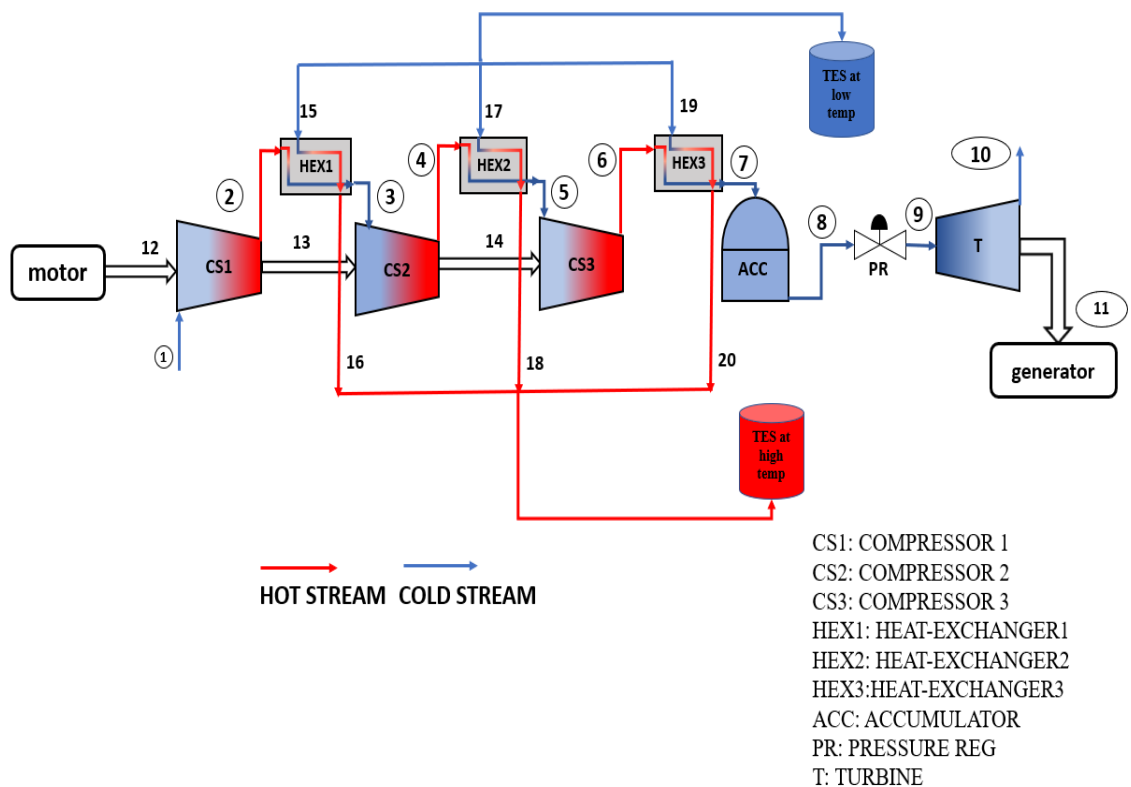
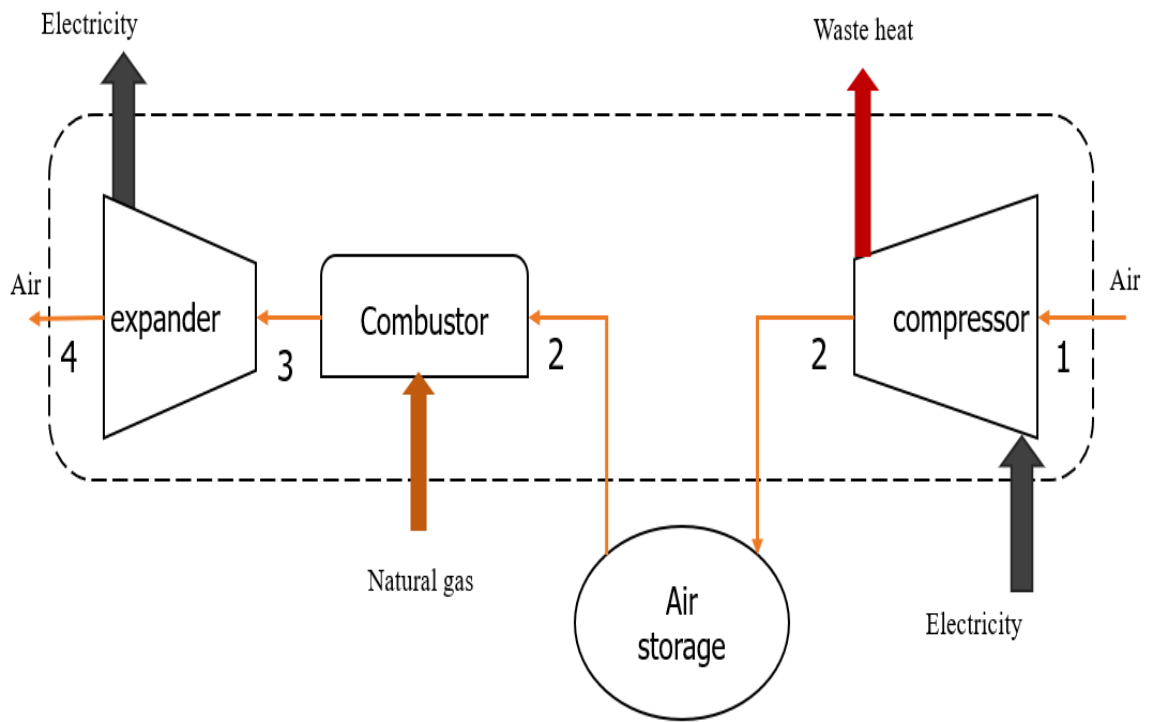
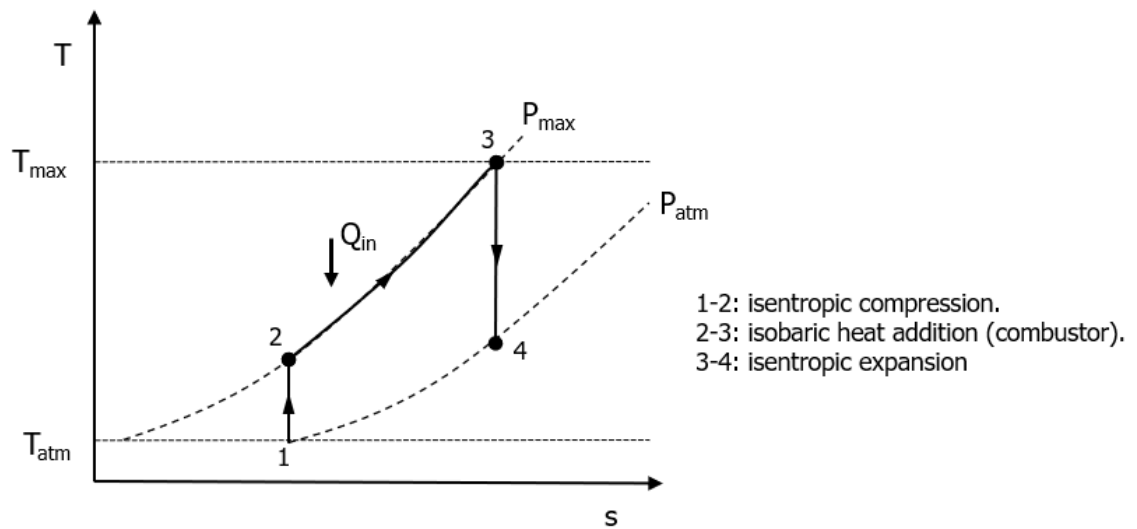


*Figure 1.2 Example of trigenerative compressed air energy storage system.*



(a)

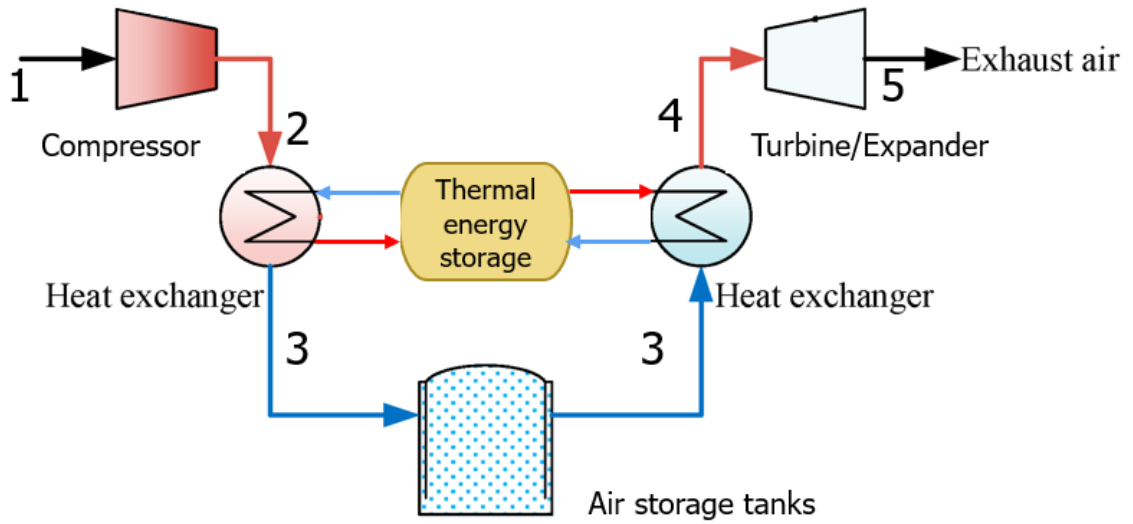


(b)

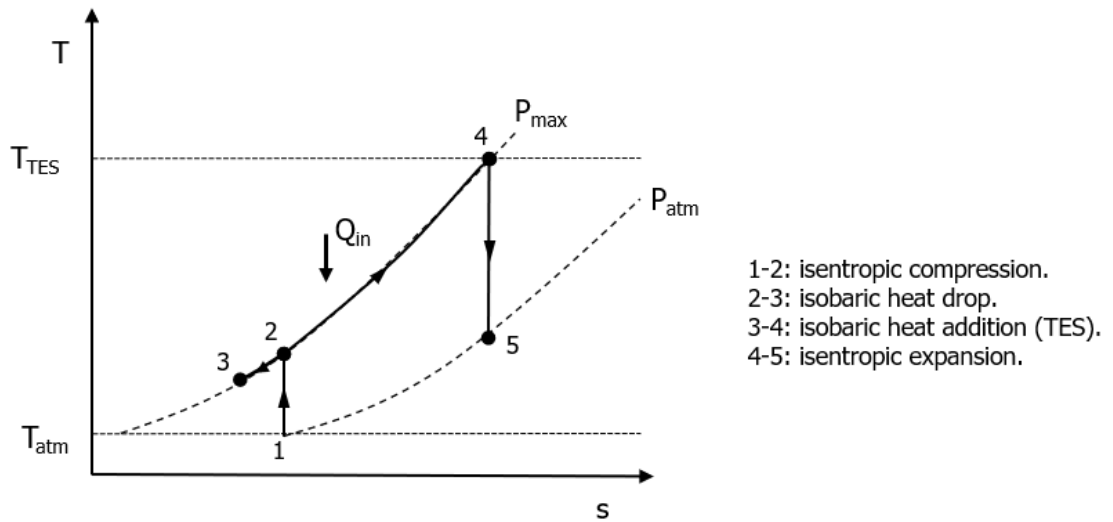
Figure 1.3 D-CAES system (a) schematic (b) T-S diagram.

A D-CAES system along with its T-S plot diagram is illustrated in [Figure 1.3](#). As you can see, isentropic compression takes place in process 1-2. This is because we are assuming ideal working conditions. The storage is considered as isobaric/adiabatic so no change in the parameters from the outlet of the storage tank. When the power is needed, discharging takes place. Isobaric heat addition takes place in process 2-3 as the air from the storage tank is pre-heated prior to expansion. Process 3-4 indicates isentropic expansion, where output air is supplied to generator to generate electricity.

An adiabatic compressed air energy storage system (A-CAES) is illustrated in [Figure 1.4 \(a\)](#) and the T-S plot for that system is shown in [Figure 1.4 \(b\)](#). Unlike D-CAES systems the heat lost by the compressor during the compression is recovered through heat-exchangers and then stored in the thermal energy storage systems. This heat is re-used for pre-heating the air before expansion. This way it reduces the use of natural gas and also reduce the emissions. Since a heat-exchanger is used after the compression to capture the heat lost. There will be slight drop in the temperature which is shown in the T-S diagram as process 2-3. Process 3-4 indicates isobaric heat-addition and 4-5 indicates the isentropic expansion.



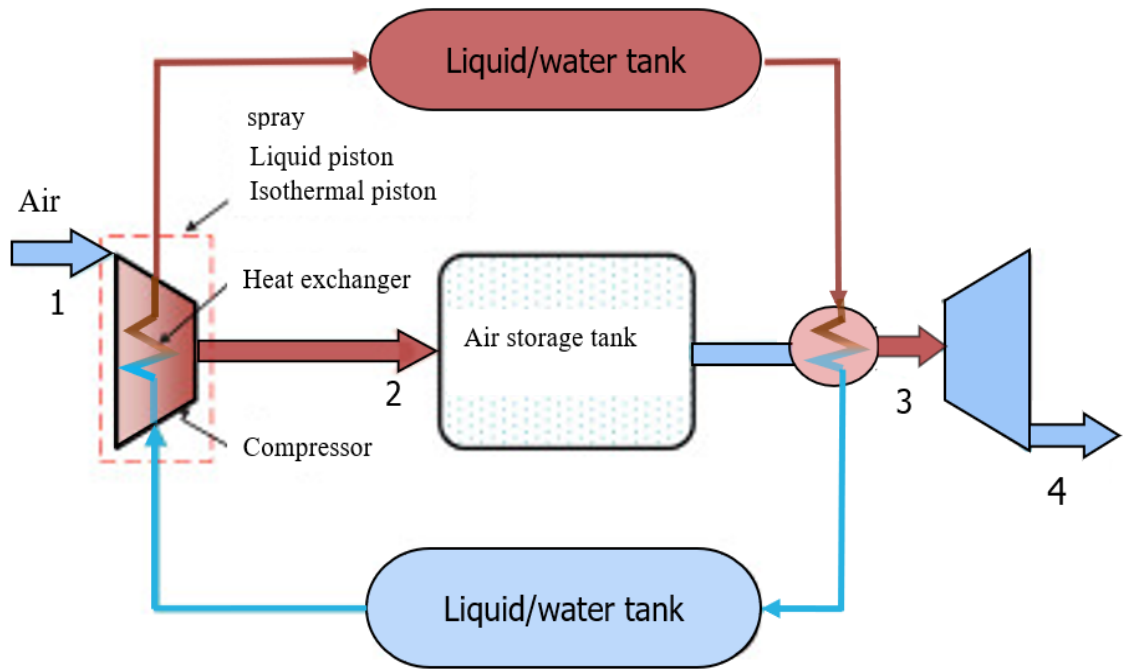
(a)



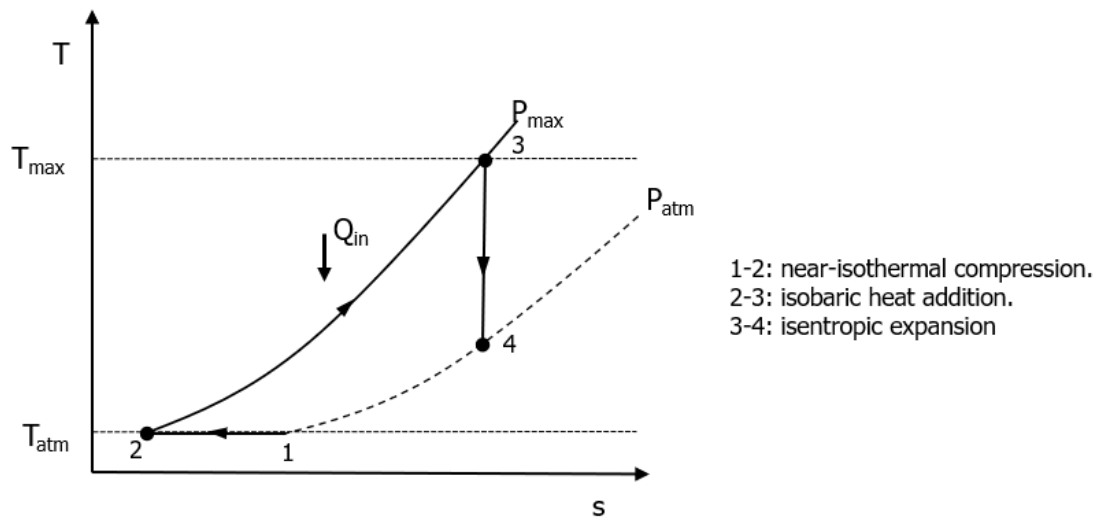
(b)

Figure 1.4 A-CAES system (a) schematic (b) T-S diagram.

The I-CAES system and its T-S plot diagram are illustrated in Figure 1.5. Main differences between isothermal CAES and adiabatic CAES are the heat transfer of the air. In case of adiabatic CAES, the temperature of the air increases significantly during air compression. High-temperature air exchanges heat with thermal stores outside compressors. In case of ICAES, the heat transfer takes place inside compressors. This allows the temperature of the air to be close to ambient during air compression, illustrated as process 1-2 in Figure 1.5 (b) indicating isothermal compression. The heat generated from the isothermal compression is reduced. The energy loss related to the heat transfer in thermal stores decreases. This eventually results in reduced power input and the increased work output. Processes 2-3 and 3-4 indicates isobaric heat-addition and isentropic expansion.



(a)



(b)

Figure 1.5 I-CAES (a) schematic (b) T-S diagram.



The current work focusses on the exergy analysis of the T-CAES system. Exergy is defined as the amount of work a system can perform when it is brought into thermodynamic equilibrium with its environment. Exergy is consumed due to irreversibility, and exergy consumption is proportional to entropy creation. The main important difference between energy and exergy is that energy is conserved, while exergy, a measure of energy quality or work potential, can be consumed. Much more detailed explanation on exergy was given in coming chapters.

### ***1.3 Literature review***

The flow chart shown in [Figure 1.6](#) summarizes the literature review. CAES research and advancement has been very active in recent years, with various aboveground and underground pilot plants being tested all over the world. Thermodynamic analysis was performed for a compressed air energy storage combined cycle (CAES-CC) by Liu et al. [12]. Zhao .P et al [13] studied a system consisting of a CAES system and a Kalina Cycle to recover waste heat was presented. The system had an efficiency higher by 4% compared to a standalone, regenerative CAES system. The overall efficiency of the system was about 10% higher than the conventional, non-regenerative reference CAES. The world's first A-CAES plant was built by HYDROSTOR in Goderich, Ontario, Canada. It stands as the first utility-scale plant with a 1.75 MW power output and a 10+ MWh storage capacity. Budt et al. [14] conducted a comprehensive literature review on CAES systems, and classified A-CAES based on the temperature level of the TES. Budt and Wolf [15] proved that a low temperature TES (below 200 °C) maintained a high level of round-trip efficiency, as well as surmounting technological problems associated with the high-temperature outputs of compressors. Zhang et al. [16] examined the effect of thermal energy storage on the efficiency of A-CAES, finding that a quantity of heat can be left in the TES which could be used to further improve the efficiency of the system. In response, Zhou et al. [17] analyzed the effect recovering the exhaust heat released from the output of the last stage turbine had on the system efficiency of A-CAES and found efficiencies approaching 68.7%.

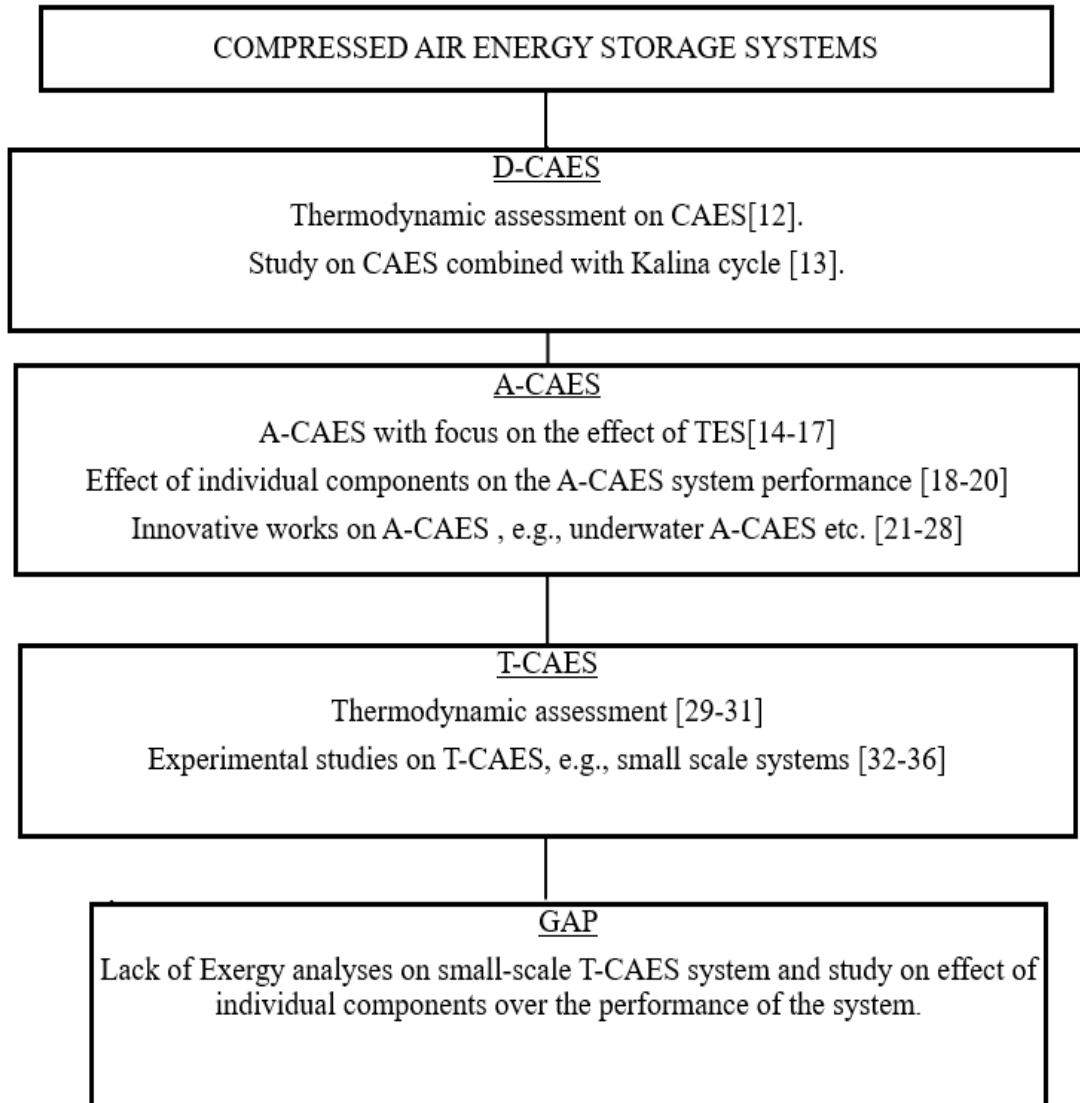


*Figure 1.6 A summary of literature review on CAES.*

Recent research has focused on the effect of compressor and turbine efficiencies on system performance. Mozayeni et al. [18] illustrated that storage pressure has a substantial effect on the amount of energy stored, concluding that increasing the efficiency of the compressors and turbines from 0.65 to 0.95 could increase the round-trip electric efficiency from 35% to 74%. In agreement with this conclusion, Luo et al. [19] established a comprehensive model for A-CAES, focusing on system efficiency optimization via a parametric analysis; the principal conclusion was that the system efficiency was dominated by the isentropic efficiency of the turbine, compressors, and the heat transfer rate of the heat exchangers. He et al. [20] studied compression phases with variable pressure ratios and optimized the compression efficiency, keeping it above 80% by varying the rotational speed and the blade inlet angle.

Many researchers have proposed innovative solutions to reduce system losses. Houssainy et al. [21] proposed a hybrid of high temperature thermal energy storage and low temperature A-CAES that included a turbocharger unit that supplements mass flow rate alongside the air storage. Their results show that the addition of the turbocharger has the potential to mitigate the required storage volume and the pressure, thus reducing the cost. Kim [22] has studied different configurations of CAES with adiabatic or quasi-isothermal compression and expansions, as well as constant volume and constant pressure air storage through energy and exergy analyses. Outcomes revealed that constant pressure and isothermal process configurations performed best of the configurations they examined.

Mazloun et al. [23] introduced an innovative constant isobaric A-CAES approach that included multistage adiabatic expansion and compression that resulted in a round-trip electrical efficiency of 53.6%.

Bagdanavicius and Jenkins [24] performed exergy analyses of a CAES system combined with hot water thermal energy storage; results revealed a 75% energy efficiency. A pilot project of underground A-CAES built in Switzerland [25,26] was studied, showing a 63% round-trip efficiency. Ebrahimi et al. [27] performed traditional and advanced exergy analyses on underwater CAES systems. Their results highlighted that 76% of destroyed exergy was avoidable, emphasizing the significant potential for improvement of the system. Transient thermodynamic modelling of an underwater compressed air energy storage system was also conducted by Carriveau et al. [28], demonstrating the significance of considering transients for the characterization and potential improvement of CAES performance.

CAES also enables the cogeneration of heat and cooling demands, which promotes the concept of T-CAES. Many configurations have been proposed which differ depending on the manner in which the compression's heat is used. Some researchers have devoted the heat produced during the charge phase for heating purposes during the discharge phase, when the electricity and the cooling energy are produced. Arabkooshar et al. [29] applied this concept to a 300 MW wind farm, proving the potential of their recommended configuration to support district heating and cooling networks. The values of power-to-power, power-to-heat and power-to-cooling efficiencies of this system were 30.6%, 92.4% and 32.3%, respectively.

Lv et al. [30] employed a thermodynamic model to assess the monthly economic and energy performance of T-CAES used for electrical energy peak load shifting at a hotel. The results showed that the trigeneration system worked efficiently at comparatively low pressures, and the efficiency

was able to reach 76.3% at 15 bars. Liu et al. [31] instituted a configuration of T-CAES and focused on the discharge process formed by a scroll expander. They evaluated its polytropic exponent as a function of the ambient temperature and examined the effects that maximum storage pressure and the expansion ratio had on the system's performance.

Additionally, there were also studies of configurations that can produce both cooling and heating energies utilizing the heat stored during the expansion process. Han and Guo [32] developed a configuration from A-CAES that enabled the liberation of cooling energy from the last stage of expansion and the delivery of excess heat as heating energy. A variable expansion ratio was proposed to increase the electric efficiency, which reached 44.5%. Li et al. [33] introduced a new tri-regenerative system to meet the end user cooling, heating, and electricity demands of a small 52 kW office building in Chicago; a global storage electric efficiency of 50% was achieved. A T-CAES system for a small-scale, standalone photovoltaic power plant with 3.7 kW electric compressor input and 1.7 kW expander electric output was proposed by Jannelli et al. [34]. The system fulfilled electric energy and cooling demand for a radio base station with a coefficient of performance (COP) of 0.62 and an electric efficiency of 57%.

Venkataramani et al. [35] constructed an experimental T-CAES setup with a wind turbine (3.2 kW), a scroll compressor, expander, and a reservoir (with a capacity of 400 L and maximum pressure of 8 bars). Increasing discharge mass flow rate increased round-trip efficiency to a maximum of 22% at the maximum flow rate. Cheayb et al. [36] performed a thermodynamic assessment of a small-scale T-CAES system. They demonstrated that the Joule-Thomson effect leads to a temperature change across the pressure regulator and that the supposition of constant

temperature is no longer true as stated in previous models of CAES systems. Their work also represented the first reliable model based on experimental data for small-scale compressed air energy storage, which will be useful for future trigenerative system studies.

Most of the literature cited above related to CAES, with focuses on theoretical modelling, system configurations and parameter optimization of T-CAES and no exergy analyses have been performed on small-scale T-CAES. Further, there has been little focus on the effect that individual components have on the whole system performance. Thus, this current work could aim to fill this gap by performing exergy analysis over the components of small-scale (4kW compressor and 2kW turbine) T-CAES which could help us in finding out the components with highest exergy destruction rate and then offering subsequent improvement recommendations. This analysis could be done by performing both standard and advanced exergy analyses. In the current work, however, we are limiting the analyses to the standard analyses.

## CHAPTER 2

### THERMODYNAMIC LAWS

A description of any thermodynamic system employs the laws of thermodynamics that form an axiomatic basis. The first law specifies that energy can be exchanged between physical systems as heat and work. The second law defines the existence of a quantity called entropy that describes the direction, thermodynamically, that a system can evolve, as well as quantifying a system's state of order. Entropy can also be used to quantify the useful work that can be extracted from the system. In this chapter, we will discuss the first and second laws of thermodynamics and how they can be employed in our CAES system.

#### ***2.1 The First Law of Thermodynamics***

The first law states that *energy can neither be created nor destroyed; it can be transformed from one form to another*. Under steady-state operation, the rate of energy entering a system is equal to that leaving the system, i.e.,

$$\text{Energy in} - \text{Energy out} = \text{Energy accumulation} \quad (1)$$

Consider an example of a compressor working under a steady-state condition with air as working fluid, as shown in [Figure 2.1](#). It is clearly observed that there is only one inlet and one exit, thus the rate of mass entering the compressor is equal to that leaving the system, i.e.,  $\dot{m}_1 = \dot{m}_2 = \dot{m}$ .



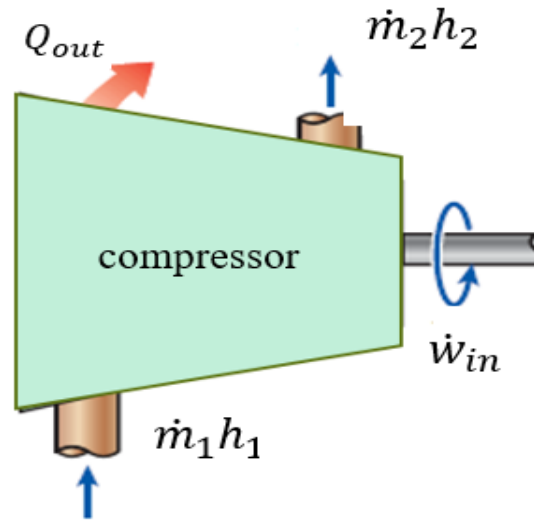


Figure 2.1 Steady state energy flow for a compressor.

Additionally, heat is lost from the system and work is supplied to the system. Under steady-state operation, the rate of energy entering the system is equal to that exiting the system, i.e.,

$$\dot{E}_{in} = \dot{E}_{out} \quad (2)$$

$$\dot{W}_{in} + \dot{m}_1 h_1 = \dot{Q}_{out} + \dot{m}_2 h_2 \quad (3)$$

Here,

$\dot{E}_{in}, \dot{E}_{out}$  = Rate of net energy transfer by heat, work, and mass

$\dot{W}_{in}$  = Rate of work input

$\dot{Q}_{out}$  = Rate of heat transfer from the system

$\dot{m}_1, \dot{m}_2$  = Mass flow rate in the system at input and output.

Energy analysis can be explained by considering the above example and Figure 2.1 for the energy flow. For our understanding input and output parameters drawn from the reference paper by Cheayb et al [36] are shown in Table 2.1. These values are required to find out the enthalpies of the working fluid i.e., air using Equation 3 as needed in the energy analysis to determine the parameters like work input etc.,

Table 2.1 Table providing the parametric data for the compressor [36].

Parameter	Value
Mass flow rate ( kg/s )	0.0039
Input pressure (bar)	1.25
Output pressure (bar)	7.7
Input temperature (°C)	23.5
Output temperature (°C)	118

## 2.2 Exergy

Exergy is consumed due to irreversibility, and exergy consumption is proportional to entropy creation. The main important difference between energy and exergy is that energy is conserved, while exergy, a measure of energy quality or work potential, can be consumed. The general exergy balance equation for any kind of process in an open or closed system is expressed as shown in the Equation 4.

$$\text{Exergy in} - \text{Exergy out} - \text{Exergy consumed} = \text{Exergy accumulation} \quad (4)$$

Exergy analysis is a very convenient method to assess the performance of energy conversion systems. It helps us to determine how a source can be used effectively [12]. It is also called the second law of thermodynamic analysis.

We considered a one-dimensional wall with steady state heat transfer, as shown in Figure 2.2 to explain the concept of exergy. To determine the total exergy destruction through this heat transfer process, we consider the system, including the regions on both sides of the wall that experience the temperature change. One side of the system boundary becomes the room temperature  $T_1$  in K, while the other side is the temperature of the outdoors  $T_2$  in K, as shown in the figure. This is a closed system, so there is no mass transfer. Here, only heat is transferred from one side to another side of the wall.

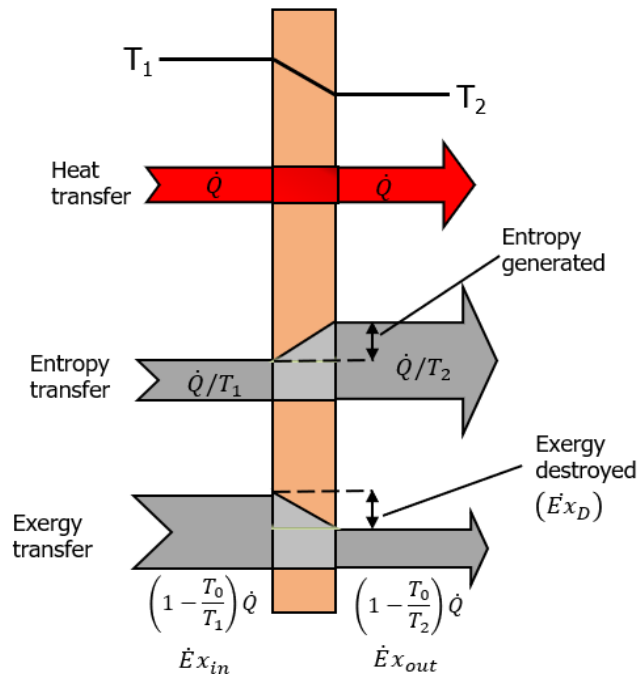


Figure 2.2 Exergy flow of steady-state heat transfer through a wall.

According to the exergy balance analysis, the amount of exergy entering the system must be equal to the amount of exergy leaving, plus the amount of exergy destroyed or consumed, as shown in Equation 5. On applying this concept to the above considered steady-state heat-transfer example, the rate of exergy destroyed is deduced as Equation 6.

$$\dot{E}_{in} - \dot{E}_{out} = \dot{E}_D \quad (5)$$

$$\dot{E}_D = \dot{Q} \left(1 - \frac{T_0}{T_1}\right)_{in} - \dot{Q} \left(1 - \frac{T_0}{T_2}\right)_{out} \quad (6)$$

where,

$$\dot{E}_{in}, \dot{E}_{out} = \text{Rate of exergy transfer by heat} = \dot{Q} \left(1 - \frac{T_0}{T}\right)$$

$$\dot{E}_D = \text{Rate of exergy destroyed}$$

$$\dot{Q} = \text{Rate of heat transfer}$$

$$T_0 = \text{Ambient temperature (K).}$$

### ***2.3 Conditions used in exergy analysis.***

Terms like *actual conditions*, *unavoidable conditions*, *relative exergy destruction* and *unavoidable exergy* which were used in the current work are discussed in this section. Also, numerical examples were given to improve understanding.

The **actual conditions** of the system are the operating conditions of the system. Here, actual efficiencies i.e., the conditions those are operating in real life are considered.

The **unavoidable working conditions** of a system are the parameters that are determined by considering the conditions under the assumption that each component operates with unavoidable thermodynamic inefficiency [13]. In more general terms, these are conditions that just cannot be predicted or avoided in the foreseeable future. The unavoidable part in the exergy destruction represents the part that cannot be eliminated even with the technological advancements available today. The advanced analysis is performed by analyzing each component separately as if the component is removed from the system. The conditions or the assumption for the advanced analysis is made considering future enhancements that can be

made for the component [42]. For this purpose, decision makers must understand the working of the entire system and rely on conditions that can improve the system. In general, it can be said that the unavoidable conditions that are considered are better than the real working conditions but are not the ideal theoretical working conditions for the component.

An explanation for both working conditions is provided by considering an example of the heat exchanger that was used in our analysis. First, the input and output parameters required by the heat exchanger under actual working conditions are shown in Table 2.2 [36]. The table displays the parameters of both working and cooling mediums. The effectiveness of the heat exchangers under actual conditions was taken as 0.583 [36].

*Table 2.2 Input and output parameters of a heat exchanger under actual conditions.*

Component	Parameter	Working fluid (air)		Cooling medium	
		In	Out	In	Out
HEX	T (K)	391	335	295	334.3
	P (bar)	7.7	6.9	1.013	1.013
	$\dot{m}$ (kg/s)	0.0039	0.0039	0.0043	0.0055

In the similar way, the input parameters and output parameters of the heat exchanger under unavoidable conditions are given in Table 2.3. These are the values those were determined by considering the highest efficiency of the component, here in this case it is the effectiveness which is considered as 0.9 [38, 42].

Table 2.3 Input and output parameters of a heat exchanger under unavoidable working conditions.

Component	Parameter	Working fluid (air)		Cooling medium	
		In	Out	In	Out
HEX	T (K)	386.2	304.1	295	359.7
	P (bar)	8.1	7.6	1.013	1.013
	$\dot{m}$ (kg/s)	0.0035	0.0035	0.0044	0.0044

Now, using the equations given, we can calculate the exergy of fuel and product, as well as the amount of exergy that was destroyed. We consider the fuel and production method to calculate exergy destroyed. The working fluid is considered to be air and the cooling medium is water. As per this method, the amount of exergy destroyed would be as shown through Equations 7, 8 and 9 [36].

$$\dot{E}_F - \dot{E}_P = \dot{E}_D \quad (7)$$

$$\dot{E}_F = \dot{m}_{c,a} \left[ c_{p,a} \cdot \left( T_{in,a} - T_{out,a} - T_{amb} \cdot \log \frac{T_{in,a}}{T_{out,a}} \right) \right] + T_{amb} \cdot R_g \cdot \log \frac{P_{in,a}}{P_{out,a}} \quad (8)$$

$$\dot{E}_P = \dot{m}_{c,w} \left[ c_{p,w} \cdot \left( T_{out,w} - T_{in,w} - T_{amb} \cdot \log \frac{T_{out,w}}{T_{in,w}} \right) \right] \quad (9)$$

where,

$\dot{m}_{c,a}$  = Mass flow rate of working fluid (air) (kg/s)

$\dot{m}_{c,w}$  = Mass flow rate of cooling fluid (water) (kg/s)

$c_{p,a}$  = Specific heat of working fluid

$c_{p,w}$  = Specific heat of cooling fluid

$\dot{E}_F$  = Exergy of fuel

$\dot{E}_P$  = Exergy of product

$R_g$  = Gas constant ( $\text{N}\cdot\text{m}\cdot\text{kmol}^{-1}\cdot\text{K}^{-1}$ )

$T_{in,a}, T_{out,a}$  = Input and output temperatures of working fluid (air) (K)

$T_{out,w}, T_{in,w}$  = Input and output temperatures of cooling fluid (water) (K)

$T_{amb}$  = Ambient temperature (K)

$P_{in,a}, P_{out,a}$  = Input and output pressures of working fluid (air).

The exergy flow in the heat exchanger is shown in [Figure 2.3](#). By using the input and output parameters provided in [Table 2.2](#) and [Table 2.3](#) and Equations [7](#) to [9](#), the amount of exergy destroyed in the heat exchanger under actual conditions and unavoidable conditions were given in [Table 2.4](#). With these results, we can understand how much amount of energy given to the system is actually utilized by the component and how much has been wasted. On the other hand, the results under unavoidable conditions help us understand how far we can improve the system by knowing the amount of exergy loss that is inevitable and the exergy loss that can be avoidable.

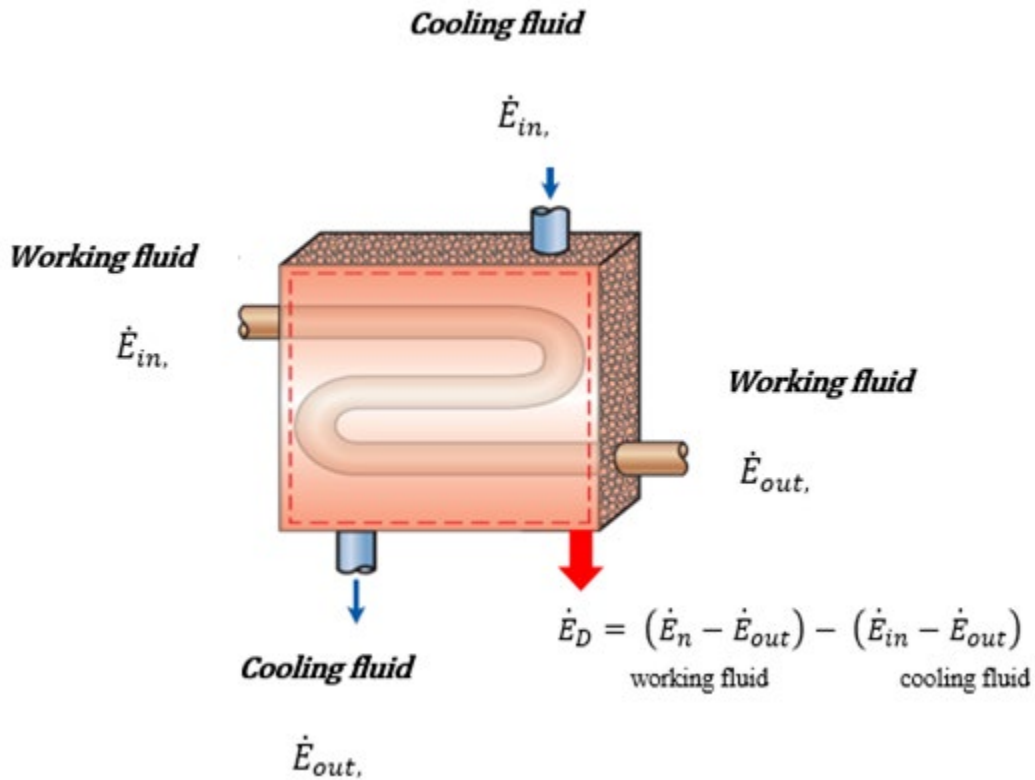


Figure 2.3 Exergy Flow in Heat-Exchanger

Table 2.4 Exergy values of the heat exchanger under actual and unavoidable conditions.

Component	Actual conditions			Unavoidable conditions		
	$E_{F,K}$ (W)	$E_{P,K}$ (W)	$E_{D\_UN}$ (W)	$E_{F,K}$ (W)	$E_{P,K}$ (W)	$E_{D\_UN}$ (W)
Heat Exchanger	41	13	27	58	38	20

A better understanding of the components can be achieved by comparing the system's performance under one condition with the performance under slightly altered conditions. Through this process, we can better see which components are more sensitive and effective for the efficiency improvement. The relative exergy destruction of a component can



be determined as ratio of difference between exergies destroyed in two state conditions to the average of those destruction rates which can be written as Equation 11.

$$E_{D\_rel} = \frac{\dot{E}_{D,K_2} - \dot{E}_{D,K_1}}{0.5 \cdot (\dot{E}_{D,K_2} + \dot{E}_{D,K_1})} \quad (10)$$

Here,

$E_{D\_rel}$  = Relative exergy destruction

$\dot{E}_{D,K_1}, \dot{E}_{D,K_2}$  = Exergy destruction at state conditions 1 and 2.

Let us consider two components – i.e., accumulator and the turbine – from our CAES system to understand the relative exergy concept. The accumulator's parameters under the first and second state conditions are illustrated in Table 2.5. Input temperature of the component has been varied by 3 degrees Celsius from the first state condition to the second state condition. Based on this change the other parameters of the component were determined. In a similar way, the two state conditions for the turbine are illustrated in Table 2.6. Upon using the exergy equations as discussed above and substituting the corresponding parameters, the relative exergies of the two components were determined and are shown in Table 2.7.

Table 2.5 Input and output parameters of an accumulator under two state conditions.

Component	Parameter	State condition 1 [36]		State condition 2	
		In	Out	In	Out
Accumulator	T (K)	306	297	309	300
	P (bar)	313.8	300	496.3	473.5
	$\dot{m}$ (kg/s)	0.0039	0.015	0.0043	0.016

Table 2.6 Input and output parameters of a turbine under two state conditions.

Component	Parameter	State condition 1 [36]		State condition 2	
		In	Out	In	Out
Turbine	T (K)	283	281.25	286	284.5
	P (bar)	5	1.013	9.48	1.5
	$\dot{m}$ (kg/s)	0.0136	0.0136	0.0144	0.0144

Table 2.7 The results of relative exergy destruction.

Component	$E_{F,K}$ (kW)	$E_{P,K}$ (kW)	$E_D$ (kW)	$E_{D\_rel}$ (kW)
Accumulator	81	78.2	2.87	0.02
Turbine	1.86	0.538	1.3	0.51

In this way, we can determine the relative exergy destruction. As mentioned, the two components were exposed to same amount of change i.e., 3<sup>o</sup> Celsius increase in the input temperature. Upon this variation imposed on the two components, one of them displayed higher relative destruction and the other one has lesser destruction. From this result, we can conclude that, it is not necessarily be the component with highest destruction rate that exhibits more sensitivity. Even components with lower destruction could exhibit higher sensitivity to the changes applied.

## CHAPTER 3

### T-CAES SYSTEM SETUP AND ANALYSES

This chapter provides a description of the system considered for these analyses and discusses the methodology of the analyses.

#### 3.1 System description

Generally, CAES has three phases: 1) charge or compression phase; 2) storage phase; and 3) the discharge or expansion process. Our system analyses are based on the previous experimental work of Cheayb et al. [36].

Figure 3.1 illustrates the schematic of the system with the charging, storing and discharge phases.

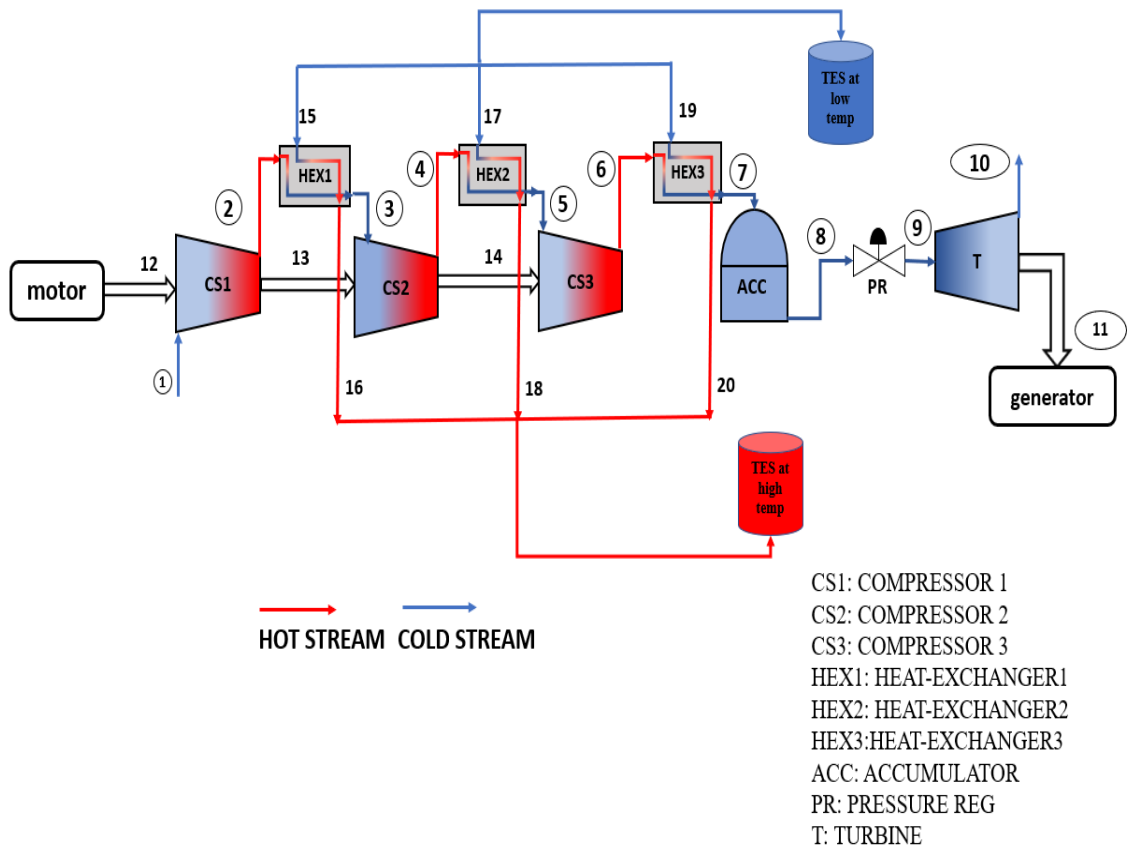


Figure 3.1 Schematic of the T-CAES system under consideration.

The six main components of trigenerative-compressed air energy storage (T-CAES) are compressors and heat exchangers for the charging phase, a storage tank for the storage phase, a pressure regulation valve, and an air motor (expander) for discharge phase and, lastly, thermal energy storage (TES). In this section, conventional exergy analyses of these components are presented, with the exception of the TES.

Here, only steady state charge and discharge phases are considered. This model is employed to evaluate both the performance of potential T-CAES configurations and prospective recommendations for improvement. The following sections discuss the thermodynamic analyses and results. The following assumptions were made to reduce modelling complexity:

1. Pressure losses at the admission, through the discharge valve, and in the heat, exchangers are not considered.
2. Compressed air is considered as a perfect gas, except in the regulating valve.
3. A constant global compression ratio is considered.
4. Kinetic and potential energies are neglected.

### **3.2 Compressors**

For limited mass flow rates and high-pressure ratios, volumetric compressors are suitable [37]. Multistage compression is required to lower the specific energy consumption for air mass storage. Inherently, volumetric compressors lose some amount of heat to the environment, which can be described by a polytropic coefficient  $\eta_c < \gamma$ . Thus, the output temperature of each stage can be calculated multiplying temperature in with the compression ratio as shown in Equation 12.

$$T_{out,c,i} = T_{in,c,i} \cdot \beta_{c,i}^{\frac{n_{c,i-1}}{n_{c,i}}} \quad (11)$$

where,

$T_{out,c,i}$  and  $T_{in,c,i}$  = Input and output temperatures of the compressor

$\beta_{c,i}$  = Compression ratio of the compressor.

The power consumption of the stage one compressor can be determined using Equation 13

$$\dot{W}_{th,c,i} = \frac{\gamma-1}{\gamma} \cdot \frac{n_{c,i}}{n_{c,i}-1} \cdot \dot{m} \cdot T_{in,c,i} \cdot C_{p,a} \cdot [\beta_{c,i}^{\frac{n_{c,i}-1}{n_{c,i}}} - 1] \quad (12)$$

where,

$\dot{W}_{th,c,i}$  = Power input to the compressor

$\dot{m}$  = Mass flow rate in the compressor.

$n_{c,i}$  = Polytropic co-efficient.

Input temperature of each stage hinges on both the previous heat exchanger and previous stage compressor's output temperature. The pressure ratio of the three compressors is constant. It should be noted that, for a fixed pressure ratio, the optimal distribution is symmetric, which is different from a manufactured compressor [37]. Air humidity is ignored because the compressor is equipped with dehumidifier.

### 3.3 Heat exchangers

Countercurrent air-to-air heat exchangers have been selected for this system. The thermal energy produced from compression is transferred from the heat source (compressed air) to the heat sink, which is the heat transfer medium. The energy balance equation for each heat exchanger can be expressed as rate of energy coming in is equal to that rate of energy leaving the component, which is shown in Equation 14.

$$\dot{Q}_{ch,i} = \dot{m}_c C_{p,i} (T_{out,c,i} - T_{in,c,i+1}) = \dot{m}_{h,w} C_{p,w} (T_{out,w} - T_{in,w}) \quad (13)$$

where,

- $\dot{Q}_{ch,i}$  = Rate of heat transfer during charging
- $\dot{m}_c$  = Mass flow rate of working fluid
- $C_{p,i}$  = Specific heat of working fluid
- $\dot{m}_{h,w}$  = Mass flow rate of heat transfer medium
- $C_{p,w}$  = Specific heat of heat transfer medium.

In this case, w denotes the heat transfer medium, which is also air.  $T_{in,w}$  denotes the temperature of incoming cooling fluid, equivalent to the ambient temperature. The heat exchanger effectiveness is expressed as ratio of actual heat-transfer to the maximum possible heat-transfer [38], Equation 15 is the ratio deduced for the current work.

$$\varepsilon_i = \frac{T_{out,c,i} - T_{in,c,i+1}}{T_{out,c,i} - T_{in,w}} \quad (14)$$

There will also be pressure loss in the heat exchangers and other components, as well. In order to facilitate the exergy analyses under unavoidable conditions, the pressure loss ratio is considered as ratio of pressure lost by the component to the pressure input to the component [38].

### 3.4 Storage Tanks

The lowest pressure of the air storage is constrained by the operating pressure of the air motor; thus, some amount of air remains in the reservoir. The air mass that could be stored is constrained by the maximum pressure permitted in the storage tank and is calculated by applying the concept of ideal gas law. Therefore, mass stored is deduced as ratio of product of pressure difference created in the tanks and volume of the tank to the temperature going into the tanks as shown in Equation 16.

$$m_s = N_{res} \frac{(P_{max} - P_{min})V_{res}}{r \cdot T_{in,res}} \quad (15)$$

where,

$m_s$  = Air mass stored in reservoir

$N_{res}$  = Number of reservoirs

$P_{max}$ ,  $P_{min}$  = Maximum and minimum pressures in the reservoir

$V_{res}$  = Volume of the reservoir

$T_{in,res}$  = Input temperature of the reservoir.

In addition, there is also some amount of air leakage from the air storage tanks, which is largely unavoidable. Thus, the air leakage in the storage tanks can be determined as the mass of air leaked out of the accumulator with respect to that remained, which is shown in Equation 17 [39]. Finally, the time required to completely charge is determined as ratio of mass stored to the rate of mass flow of the working fluid which can be expressed as Equation 18.

$$\omega = \frac{m_{leak}}{m_{in,acc}} \quad (16)$$

$$t = \frac{m_s}{\dot{m}_c} \quad (17)$$

There are a few assumptions made during the storage phase, and they are as follows.

1. The temperature gradient inside the storage tank is insignificant.
2. The heat capacity of the compressed air is constant, independent of the pressure variation.
3. The thermal resistance of the wall thickness is insignificant compared to the resistance due to natural convection.

### 3.5 Turbine

The discharge time is calculated as ratio of mass stored to the mass flowrate of working fluid in expansion phase which can be seen in Equation 19 [36].

$$t_{dis} = \frac{m_s}{\dot{m}_e} \quad (18)$$

For small-scale applications, an open research question remains over the best expander to choose between volumetric (piston) and high-speed axial turbines [40]. Volumetric expanders like scroll machines exhibit high performance but are restricted to small pressure variations [40]. Piston expanders are advantageous for most CAES systems where high pressures would be expected. Cheayb et al. opted for piston expanders, hence, we also considered the same type. Through correlation with compression, the thermodynamic power and the output temperature of the ideal expansion cycle are obtained from Equations 20 and 21.

$$T_{out,e} = T_{in,e} \cdot \beta_d^{\frac{1-n_e}{n_e}} \quad (19)$$

$$\dot{W}_{th,e} = \frac{\gamma-1}{\gamma} \cdot \frac{n_e-1}{n_e} \cdot \dot{m}_e \cdot T_{in,e} \cdot C_{p,a} \cdot \left[ 1 - \beta_d^{\frac{1-n_e}{n_e}} \right] \quad (20)$$

where  $\beta_d$  = Expansion ratio in the turbine

$T_{in,e}, T_{out,e}$  = Input and output temperatures of the compressor

$\dot{W}_{th,e}$  = Rate of work done by the turbine

$\dot{m}_e$  = Mass flow rate through the turbine.

$n_e$  = Polytropic co-efficient.

Both input pressure and the temperature of the expansion valve are equal to the values of the storage tank and decrease with time. However, the current work is limited to steady state conditions only. The thermodynamic or pneumatic mechanical efficiency is introduced to account for the deviation



between actual and ideal thermodynamic cycles and mechanical losses. This efficiency can be expressed as ratio of mechanical shaft power to the thermodynamic power as shown in Equation 22.

$$\eta_{th} = \eta_m \cdot \eta_{th} = \frac{\dot{W}_{m,e}}{\dot{W}_{th,e}} \quad (21)$$

where,

$\eta_{th}$  = Thermodynamic efficiency

$\eta_m$  = Mechanical efficiency.

$\dot{W}_{m,e}$  = Mechanical shaft power.

$\dot{W}_{th,e}$  = Thermodynamic power.

### 3.6 Thermodynamic (Exergy) analyses

To analyze the performance of the T-CAES system comprehensively, exergy analyses are executed to determine the sources, location, and extent of the exergy destruction. The exergy of a system at a certain thermodynamic state is the maximum amount of work that can be obtained when the system moves from that particular state to a state of equilibrium with its surroundings; exergy losses relate to lost work. In order to perform these analyses, an exergy balance equation is built for each component [41]. The mass balance, energy and exergy balance equations for each component of a system can be written as shown in Equations 23, 24 and 25.

$$\text{Mass balance:} \quad \sum \dot{m}_{in} - \sum \dot{m}_{out} = 0 \quad (22)$$

$$\text{Energy balance:} \quad Q - W = \sum \dot{m}_{out} \cdot h_{out} - \sum \dot{m}_{in} \cdot h_{in} \quad (23)$$

$$\text{Exergy balance:} \quad Q - W = \sum \dot{m}_{out} \cdot e_{out} - \sum \dot{m}_{in} \cdot e_{in} + E_D \quad (24)$$

where Q is the heat transfer rate (kW) to the control volume, W is the rate of work leaving the control volume (kW), m is the mass flow rate (kg/s), h is the specific enthalpy (kJ/kg), e is the specific exergy (kJ/kg) and  $E_D$  is the exergy destruction rate.

Thermomechanical exergy and chemical exergy are the two terms to express the overall exergy of the system [3]. Since our system has no chemical reaction, the chemical exergy is zero. The thermomechanical exergy is the extreme amount of effective energy. Therefore, the total exergy of the fluid stream is equal to the product mass flowrate and specific exergy which is shown in Equation 26.

$$\dot{E} = \dot{m} \cdot e \quad (25)$$

The expression for specific exergy is as given in Equation 27.

$$e = (h - h_0) - T_0(s - s_0) \quad (26)$$

where  $h_0$  and  $s_0$  are the specific enthalpy and specific entropy, respectively, at the ambient environmental condition.  $T_0$  is the environment temperature. We need temperature  $T$  and pressure  $P$  under actual conditions to determine enthalpy, entropy, and exergy. These parameters for actual conditions are taken from Cheayb [36], in which they determined by experimental setup.

The same parameters are calculated for the unavoidable working conditions by considering additional assumptions, like efficiencies and losses in the system, as shown in the Table 3.1.

Table 3.1 Parametric considerations.

COMPONENTS	PARAMETERS	ACTUAL CONDITIONS [36]	UNAVOIDABLE CONDITIONS
CS1	Isentropic efficiency	85%	95% [37, 42]
	Compression ratio	7.0	8.0
CS2	Isentropic efficiency	85%	95% [37, 42]
	Compression ratio	7.0	8.0
CS3	Isentropic efficiency	85%	95%
	Compression ratio	7.0	8.0
HX1	Effectiveness	0.58	0.9 [38, 42]
	Air pressure loss	1.2 kPa	$0.38 \cdot \Delta p_{\text{actual}}$ [27]
HX2	Effectiveness	0.796	0.9 [38, 42]
	Air pressure loss	1.2 kPa	$0.38 \cdot \Delta p_{\text{actual}}$ [27]
HX3	Effectiveness	0.83	0.9 [38, 42]
	Air pressure loss	1.2 kPa	$0.38 \cdot \Delta p_{\text{actual}}$ [27]
ACC	Air leak ratio	35%	10%
PR	Pressure loss ratio	0.98	0.3
	Air leak ratio	0.1	0.02
T	Isentropic efficiency	85%	95% [36]

### 3.7 Analysis methodology

The exergy equations were developed for each component based on the fuel and product concept. For the complete conventional exergy analyses of

the  $k_{th}$  component of the small-scale T-CAES system, the variables such as exergy destruction, exergy efficiency and exergy destruction ratio are delineated in Equations 28, 29 and 30. Where exergy destroyed is defined as the difference between exergy of fuel and the exergy of product, exergy efficiency is defined as the ratio of exergy of product to the exergy of fuel and destruction ratio is defined as ratio of amount of exergy destroyed to the exergy of fuel.

$$\dot{E}_D = \dot{E}_{F,K} - \dot{E}_{P,K} \quad (27)$$

$$E_{eff} = \frac{\dot{E}_{P,K}}{\dot{E}_{F,K}} \quad (28)$$

$$y_k = \frac{\dot{E}_{D,K}}{\dot{E}_{F,K}} \quad (29)$$

In the above equations,  $E_D$  is the amount of exergy destroyed,  $E_{F,K}$  is the exergy of fuel and  $E_{P,K}$  is the exergy of the product. Also,  $y_k$  and  $E_{eff}$  are the exergy destruction ratio and exergy efficiency, respectively. To determine  $E_D$ , the energy and exergy balances are essential. In Table 3.2, these equations are delineated for each component of the small-scale trigenerative compressed air energy storage systems. The total exergy efficiency of the system is determined as the ratio of total product exergy to the total amount exergy destroyed on fuel side which is shown in Equation 31.

$$\varepsilon_{tot} = \frac{\dot{E}_{P,tot}}{\dot{E}_{F,tot}} \quad (30)$$

In the above equation,  $E_{p, tot}$  is the exergy delivered to the grid and  $E_{F, tot}$  is the total exergy entering the system. Also, a better understanding of the components is achieved by comparing the performance of the system under one condition with its performance under conditions that are altered slightly. Through this process, we can better see which components are more

sensitive and effective for the efficiency improvement. Equation 32 for relative exergy destruction, is used for comparing the results under actual and unavoidable working conditions.

$$Ex_{rel} = \frac{E_{D,K,2} - E_{D,K,1}}{0.5 \cdot (E_{D,K,2} + E_{D,K,1})} \quad (31)$$

where  $Ex_{rel}$  = Relative exergy destruction

$E_{D,K,1}$  = Exergy destruction of the component at state condition 1

$E_{D,K,2}$  = Exergy destruction of the component at state condition 2.

Table 3.2 Energy and exergy balance equations for the components of the system.

Components	Energy Balance Equations	Exergy Balance Equations
		$E_{D,K} = (E_{F,K}) - (E_{P,K})$
CS1	$W_{CS1} = \dot{m}_1 (h_2 - h_1)$	$E_{D,K} = (E_{12}) - (E_2 - E_1)$
HX1	$\eta_{HX1} \cdot \dot{m}_2 (h_2 - h_3) = \dot{m}_{15} (h_{16} - h_{15})$	$E_{D,K} = (E_2 - E_3) - (E_{16} - E_{15})$
CS2	$W_{CS2} = \dot{m}_3 (h_4 - h_3)$	$E_{D,K} = (E_{13}) - (E_4 - E_3)$
HX2	$\eta_{HX2} \cdot \dot{m}_4 (h_4 - h_5) = \dot{m}_{17} (h_{18} - h_{17})$	$E_{D,K} = (E_4 - E_5) - (E_{18} - E_{17})$
CS3	$W_{CS3} = \dot{m}_5 (h_6 - h_5)$	$E_{D,K} = (E_{14}) - (E_6 - E_5)$
HX3	$\eta_{HX3} \cdot \dot{m}_6 (h_6 - h_7) = \dot{m}_{19} (h_{20} - h_{19})$	$E_{D,K} = (E_6 - E_7) - (E_{20} - E_{19})$
ACC	$\dot{m}_7 \cdot h_7 = \dot{m}_8 \cdot h_8$	$E_{D,K} = E_7 - E_8$
PR	$\dot{m}_8 \cdot h_8 = \dot{m}_9 \cdot h_9$	$E_{D,K} = E_8 - E_9$
T	$W_{TUR} = \dot{m}_9 (h_{10} - h_9)$	$E_{D,K} = (E_{10} - E_9) - (E_{11})$

## CHAPTER 4

### RESULTS AND DISCUSSIONS

This chapter describes the major results from the analyses and the conclusions that can be formed from them. The following sections also discuss the recommendations and future works that can be considered.

#### *4.1 Results and Discussions*

The thermodynamic performance (exergy) analyses have been carried out for the proposed system. The main thermodynamic properties under actual and unavoidable working conditions are shown in [Table 4.1](#). Also, in [Table 4.2](#), thermodynamic properties are given for state point 2 (where the parameters differ slightly from the properties under actual and unavoidable conditions in state point 1). Two state points were considered for each condition in order to determine which component is more sensitive to the changes. Even though a specific component exhibits a higher exergy destruction, it might be another component that is showing more sensitivity to the changes in its conditions. For the system considered here, the exergy analyses under actual conditions shows that more than half of the total exergy destruction is caused by the accumulator. This loss occurs over both the charge and discharge phases. About a quarter of the destruction is caused by the pressure regulator and turbine. Further, the analysis under unavoidable conditions reveals that the pressure regulator, turbine, and accumulator offer 65.7%, 32.3% and 27% recoverable exergies, respectively; these contribute to a 35% increase in overall exergy efficiency of the system. This result indicates that there is great potential for improvement. The results for the exergy analyses of the proposed T-CAES system under actual and unavoidable working conditions are delineated in

Table 4.3 and Table 4.4. These results were computed in MATLAB using Equations 28 to 31.

*Table 4.1 Parameters at first condition calculated using Equations 12 to 21*

State point	Fluid	Actual conditions			Unavoidable conditions		
		T (K)	P (bar)	m (kg/s)	T (K)	P (bar)	m (kg/s)
1	Air	296.5	1.25	0.0039	296.5	1.25	0.0035
2	Air	391	7.7	0.0039	386.2	8.1	0.0035
3	Air	335	6.5	0.0039	304.12	7.6	0.0035
4	Air	471.7	44.4	0.0039	434.9	45.6	0.0035
5	Air	331	43.2	0.0039	310.65	45.1	0.0035
6	Air	425	315	0.0039	399.9	320.2	0.0035
7	Air	306	313.8	0.0039	305.4	319.4	0.0035
8	Air	297	300	0.015	303.4	313.0	0.0189
9	Air	183	5	0.0136	300.3	219.1	0.0185
10	Air	281.52	1.013	0.0136	281.4	54.7	0.0185
15	Air	295	1.013	0.0055	295	1.013	0.0044
16	Air	334.7	1.013	0.0055	359.7	1.013	0.0044
17	Air	295	1.013	0.0055	295	1.013	0.0044
18	Air	394.3	1.013	0.0055	392.2	1.013	0.0044
19	Air	295	1.013	0.0055	295	1.013	0.0044
20	Air	379.3	1.013	0.0055	369.6	1.013	0.0044

Table 4.2 Parameters at second condition calculated using Equations 12 to 21

State point	Fluid	Actual conditions			Unavoidable conditions		
		T (K)	P (bar)	m (kg/s)	T (K)	P (bar)	m (kg/s)
1	Air	296.5	1.25	0.0043	296.5	1.25	0.0041
2	Air	394	11.4	0.0043	389.2	12	0.0041
3	Air	338.1	10.2	0.0043	307.12	11.5	0.0041
4	Air	474.1	69.4	0.0043	436.9	69.2	0.0041
5	Air	33.9	68.2	0.0043	313.7	68.7	0.0041
6	Air	427.9	497.5	0.0043	402.9	488.1	0.0041
7	Air	309	496.3	0.0043	308.4	487.5	0.0041
8	Air	300	474.5	0.016	306.4	477.7	0.0225
9	Air	286	9.48	0.0144	303.3	334.4	0.022
10	Air	284.5	1.5	0.0144	284.4	83.5	0.022
15	Air	298	1.5	0.0055	298	1.5	0.0044
16	Air	341.7	1.5	0.0055	374.5	1.5	0.0044
17	Air	298	1.5	0.0055	298	1.5	0.0044
18	Air	407.5	1.5	0.0055	412.8	1.5	0.0044
19	Air	298	1.5	0.0055	298	1.5	0.0044
20	Air	390.9	1.5	0.0055	386.1	1.5	0.0044



*Table 4.3 Results of the exergy analyses of small-scale T-CAES under actual working conditions calculated using Equations 28 to 32*

<b>Component</b>	$\dot{E}_{F,K}$ (kW)	$\dot{E}_{P,K}$ (kW)	$\dot{E}_D$ (kW)	$\dot{E}_{D\_rel}$ (kW)	$E_{eff}$ (%)	$Y$ (%)
<b>CS1</b>	1.01	0.722	0.287	0.11	70	28.4
<b>CS2</b>	1.06	0.778	0.238	0.31	72.9	22.4
<b>CS3</b>	1.1	0.737	0.363	0.11	66.9	33
<b>HX1</b>	0.041	0.013	0.027	0.88	33	65.8
<b>HX2</b>	0.145	0.077	0.067	0.07	53	46.2
<b>HX3</b>	0.088	0.057	0.031	0.06	64	35.2
<b>ACC</b>	81	78.2	2.87	0.02	21	35.4
<b>PR</b>	7.3	4.91	2.39	0.03	26.6	73.9
<b>TUR</b>	1.86	0.538	1.3	0.51	28	69.8

*Table 4.4 Results of the exergy analyses of small-scale T-CAES under unavoidable working conditions calculated using Equations 28 to 32*

<b>Component</b>	$\dot{E}_{F,K}$ (kW)	$\dot{E}_P$ (kW)	$\dot{E}_D$ (kW)	$\dot{E}_{D\_rel}$ (kW)	$E_{eff}$ (%)	$Y$ (%)
<b>CS1</b>	0.936	0.659	0.277	0.16	71	29.6
<b>CS2</b>	0.829	0.620	0.195	0.18	78	21.7
<b>CS3</b>	0.931	0.634	0.293	0.18	69.6	30.3
<b>HX1</b>	0.058	0.028	0.03	0.28	46	53.3
<b>HX2</b>	0.107	0.059	0.04	0.24	64.7	34.7
<b>HX3</b>	0.062	0.036	0.015	0.32	66.9	33.3
<b>ACC</b>	81.23	79.6	1.63	0.08	42.3	10.3
<b>PR</b>	9.31	8.55	0.763	0.19	51	8.2
<b>TUR</b>	2.19	1.37	0.82	0.18	53.4	37.6

The tabled results confirm the dominant role played by the accumulator in the sum of exergy destruction (more than half). This loss is due to significant air leakage in the high-pressure, low-temperature storage tanks. Nearly 35% of air leakage is happening under actual conditions. Under unavoidable working conditions, the storage tanks also exhibit high exergy destruction. The fuel and product exergies associated with the accumulator are relatively higher than the other components in the system, which can be seen in [Table 4.3](#). The second and third highest exergy destruction rates occur in the pressure regulator and the turbine, respectively, with corresponding values of 2.39 and 1.3 kW. The high exergy destruction rate in the turbine is due to the low isentropic efficiency in the low-pressure turbine; significant losses from the pressure regulator also notably contribute to exergy destruction. Meanwhile, under unavoidable conditions, the exergy destruction rates of these components decreased to levels below the actual condition values. There is not much difference in the component-wise order of destruction rates, as it follows the same order as in actual working conditions.

In terms of exergy efficiencies (shown in [Figure 4.1](#)), though the accumulator shows the highest amount of exergy destruction, it is the pressure regulator that demonstrates a great potential for improvement. This is revealed by the exergy efficiency of the pressure regulator increasing from 26.6% under the actual condition to 51% under the unavoidable condition. It is clear that the exergy efficiencies of the components under unavoidable conditions are higher than those under actual conditions. The compressors and the pressure regulator exhibit higher exergy efficiencies than the heat exchangers, even though they have high exergy destruction rates when compared to heat exchangers. This finding indicates that the amount of fuel

exergy destroyed in the heat exchangers is relatively higher than the exergy destroyed on the product side. The increase in overall system exergy efficiency from 17% to 51.3% indicates significant potential for improvement.

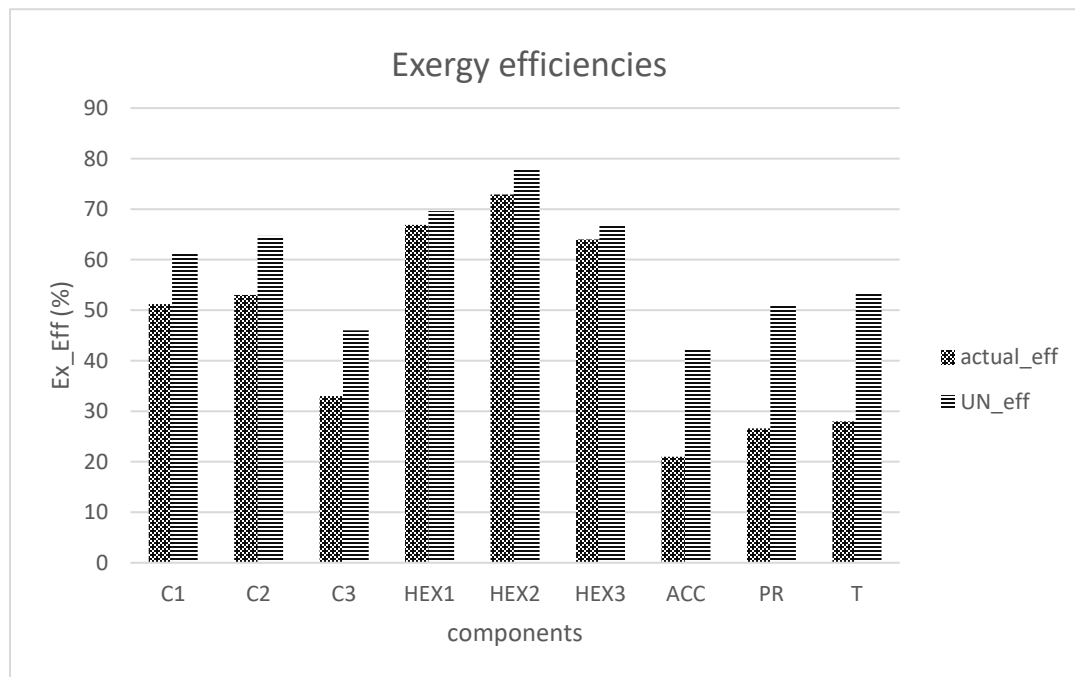


Figure 4.1 Figure illustrating the exergy efficiencies under two working conditions.

Table 4.5 Results of accumulator.

Component	Exergy destroyed		Exergy efficiency	
	$\dot{E}_D$ (kW)	$\dot{E}_{D\_UN}$ (kW)	$E_{eff}$ (%)	$E_{eff\_un}(\%)$
Acc	2.87	1.63	21	42.3

The tabled results confirm the dominant role of the accumulator in the sum of exergy destruction, as it was responsible for more than half. This loss is due to significant air leakage in the high-pressure, low-temperature storage tanks. Nearly 35% of air leakage is happening under actual conditions. Under unavoidable working conditions, the storage tanks also exhibit high exergy destruction. The fuel and product exergies associated with the accumulator are relatively higher than the other components in the system.

The relative exergy destruction determined using Equation 36 for different components of the small-scale T-CAES system under actual and unavoidable working conditions are shown in Figure 4.2. Relative exergy destruction helps us to identify which component is sensitive among multi-stage components and also in the overall system to the changes imposed. In the present work we have multi-stage compressors and the heat-exchangers. Among the three compressors, compressor stage 2 displayed more sensitivity followed by compressor stage 3 and stage 1 under actual working conditions. Whereas unavoidable conditions stage 2 and 3 compressors show similar sensitivity. Among the heat-exchangers the order of sensitivity under actual conditions is HEX1, HEX2 and HEX3 with the destruction values of 0.88, 0.07 and 0.04. But the order changes under unavoidable conditions with HEX3 taking the first position followed by HEX1 and HEX2, respectively. When we consider the entire system, turbine is also showing higher sensitivity to the changes given.

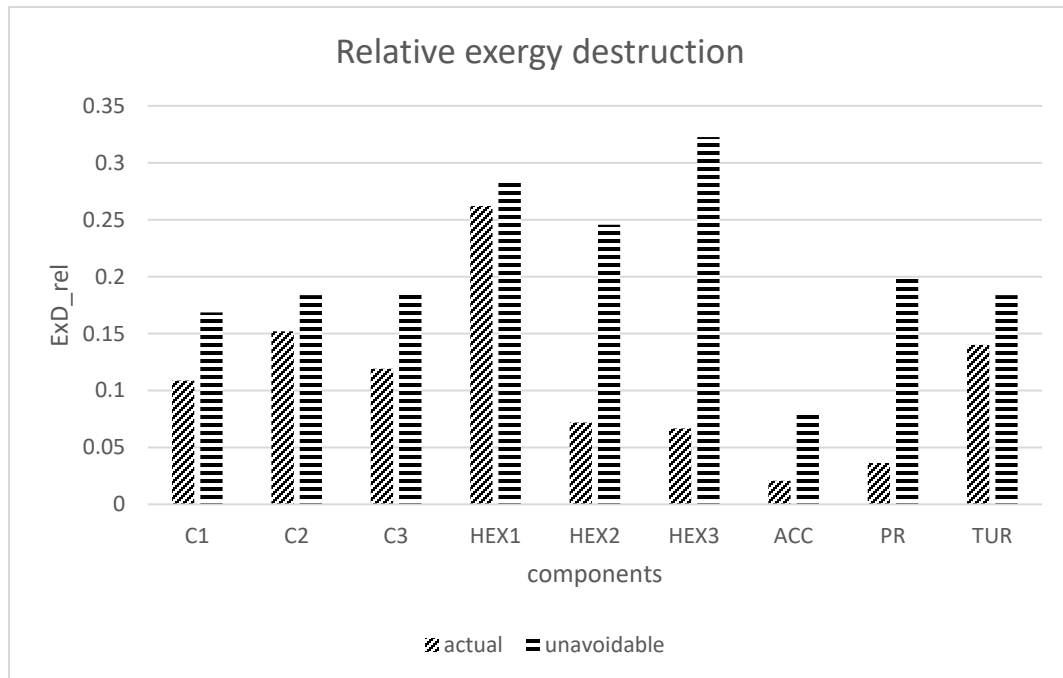


Figure 4.2 Figure illustrating the relative exergy under two working conditions.

In terms of exergy destruction ratios under actual working conditions – as shown in Figure 4.3– the pressure regulator has the highest exergy destruction ratio (73.6%) under actual conditions. This means that 73.6% of the exergy of fuel entering the pressure regulator is destroyed through direct contact with environment. The turbine and heat exchangers 1 and 2 have the second, third and fourth highest destruction ratios under actual working conditions, with values of 69%, 65.8% and 46%, respectively. High exergy destruction ratios in heat exchangers are due to large temperature differences between hot and cold streams. Under unavoidable conditions, there is a change in the order of the destruction ratios illustrated in Figure 4.4. Here, heat exchanger 1 has the highest exergy destruction ratio with 63.5%, followed by the turbine with 38% and heat exchanger 2 with 37.3%. The pressure regulator’s destruction ratio has reduced from 73.6% to 8.9%, showing notable opportunity for improvement.

This result tells us that significant exergy can be conserved if the air leakage and pressure losses are reduced. There is also a significant decrease in the overall exergy destruction ratio, as shown in [Figure 4.5](#).

Finally, improvement priority order is given in [Table 4.6](#). This order is based on the exergy destruction values of the components determined using defined equations. Under actual working conditions, accumulator should be given the top priority, followed by the pressure regulator and the turbine. Whereas, under unavoidable working conditions the first priority is taken by accumulator again followed by a slight change as turbine displayed higher destruction than pressure regulator. Hence, second priority is to turbine followed by pressure regulator and the compressors stage 3, 1 and 2. From this result we can improve our actual focusing more on the top priority components.

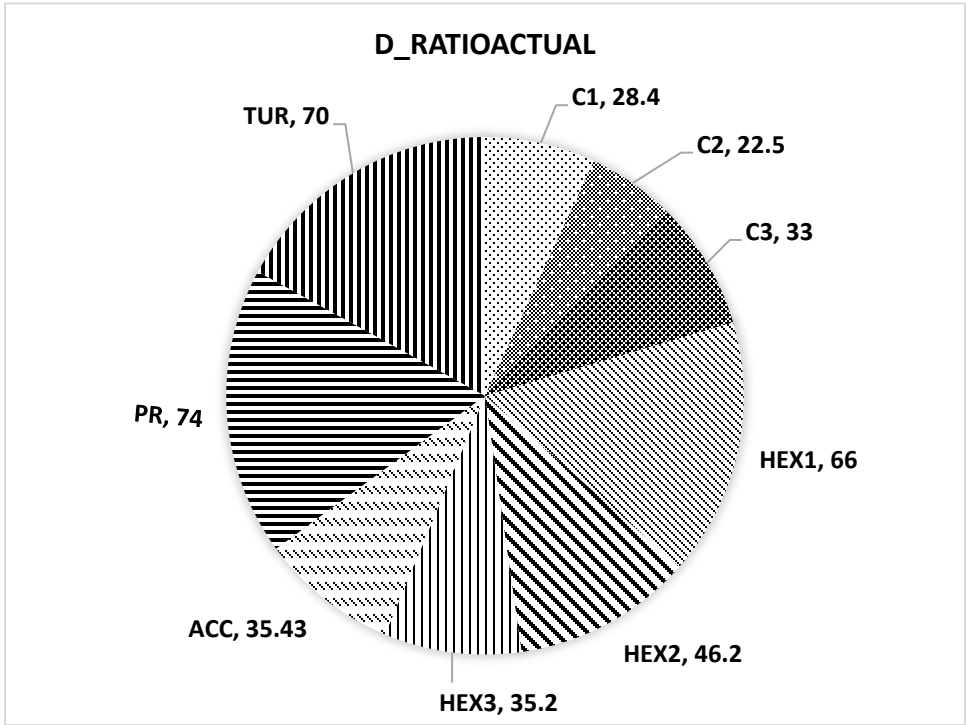


Figure 4.3 Exergy destruction ratio under actual conditions

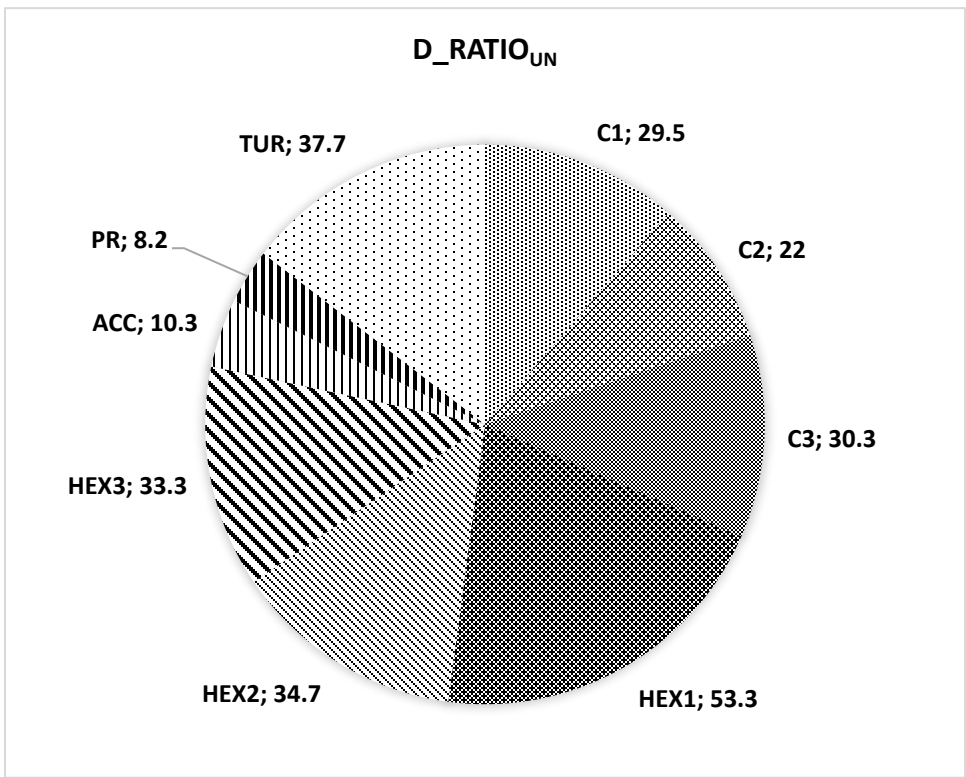


Figure 4.4 Exergy destruction ratio under unavoidable condition

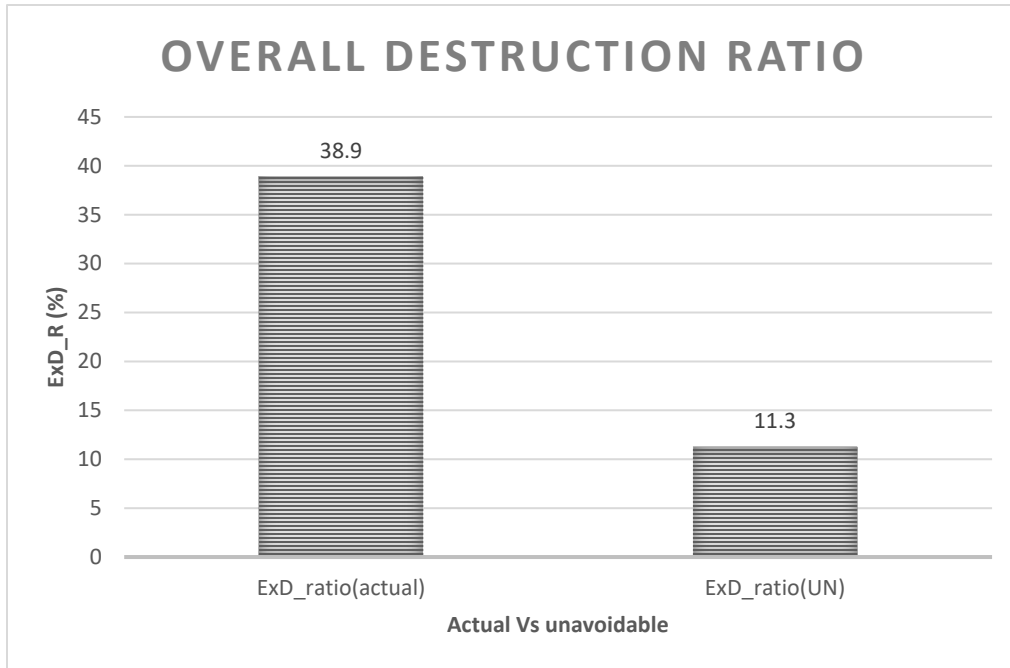


Figure 4.5 Overall exergy destruction of the system.

Table 4.6 Improvement priority order for the components.

Rank	Actual conditions		Unavoidable conditions	
	Component	$E_D$	Component	$E_D$
1	HEX1	0.287	HEX3	0.277
2	TUR	0.238	HEX1	0.195
3	CS2	0.363	HEX2	0.293
4	CS3	0.027	PR	0.03
5	CS1	0.067	CS3	0.04
6	HEX2	0.031	TUR	0.015
7	HEX3	2.87	CS2	1.63
8	PR	2.39	CS1	0.763
9	ACC	1.3	ACC	0.82



## **CHAPTER 5**

### **CONCLUSIONS**

Exergy analyses are performed on a small-scale (4kW compressor and 2kW turbine) trigenerative compressed air energy storage system, which was proposed in experimental form by Cheayb et al. Our principal conclusions are as follows.

- Results suggest that, in the proposed T-CAES system, the individual components offer a significant number of recoverable exergies, which have increased the overall exergy efficiency of the system under consideration by 35%.
- The largest quantity of exergy is destroyed in the accumulators under both actual and unavoidable working conditions. There is a significant reduction, however, in the amount of exergy destroyed in accumulators from the actual to the unavoidable conditions.
- Even though the accumulators show high exergy destruction, it was revealed that, in terms of destruction ratio, the pressure regulator shows the highest (73.1%) under actual working conditions and 8.2% under unavoidable conditions. These numbers suggest that the pressure regulator has a high fuel exergy destruction under actual conditions. Under unavoidable conditions, though, heat exchanger 1 displays a high destruction ratio of 63.5%. With this finding, we can conclude that, even though a specific component exhibits a high destruction rate, it will not necessarily be the same component with the highest potential for improvement.
- Calculating relative exergy destruction of each of the k-th components of the system enabled systematic sensitivity analyses that helped

determine which components would be most affected by parametric change.

Future work will look to optimize the system configuration and actual parameters. A steady state condition was considered for this system, as it is informative and straightforward to implement, but can be limiting when the compression ratio varies. In our future work, the transient nature of the discharge phase will be accounted for to better assess the cooling potential and the output power. We will also execute more detailed, “advanced” exergy analyses. This will improve the identification of changes required to improve system performance. Avoidable and unavoidable conditions will be considered in these advanced analyses. Finally, a few potential improvement strategies, mentioned below, could be used in future work to reduce the losses in the pressure regulator, which, in turn, improves the overall system performance.

- Increasing the expansion ratio to 25 by introducing the recently developed micro-turbines [38].
- Replacing the throttling valve with a Ranque-Hilsch vortex tube or a cascade of vortex tubes. These devices have the capability to relax the air to reduce the maximum inlet pressure allowed by current microturbines, while producing a hot and a cold stream. The produced cooling power would be then reinjected within some heat exchangers of the compressed air energy storage system towards improved efficiency.

## REFERENCES/BIBLIOGRAPHY

1. Luo, X., Wang, J., Dooner, M., & Clarke, J. (2015). Overview of current development in electrical energy storage technologies and the application potential in power system operation. *Applied Energy*, 137, 511-536.
2. *Global Energy Statistical Yearbook 2020*, (2020). Enerdata. <https://yearbook.enerdata.net/world4electricity-production-map-graph-and-data.html>.
3. Barbour, E., Mignard, D., Ding, Y., & Li, Y. (2015). Adiabatic compressed air energy storage with packed bed thermal energy storage. *Applied Energy*, 155, 804-815.
4. Chen, H., Cong, T. N., Yang W., Tan, C., Li, Y., & Ding, Y. (2009). Progress in electrical energy storage system: A critical review. *Progress in Natural Science*. 19(3), 291-312.
5. Ebrahimi, M., Carriveau, R., Ting, D. S., & McGillis, A. (2019). Conventional and advanced exergy analyses of a grid connected underwater compressed air energy storage facility. *Applied Energy*, 242, 1198-1208.
6. Guo, C., Pan, L., Zhang, K., Oldenburg, C. M., Li, C., & Li, Y. (2016). Comparison of compressed air energy storage process in aquifers and caverns based on the Huntorf CAES plant. *Applied Energy*, 181, 342-56.
7. Luo, X., Wang, J., Krupke, C., Wang, Y., Sheng, Y., Li, J., Xu, Y., Wang, D., Miao, S., & Chen, H. (2016). Modelling study, efficiency analyses and optimization of large-scale Adiabatic Compressed Air Energy Storage systems with low-temperature thermal storage. *Applied Energy*, 162, 589-600.
8. Yu, Q., Wang, Q., Tan, X., Fang, G., & Meng, J. (2019). A review of compressed-air energy storage. *Journal of Renewable and Sustainable Energy*. 11(4), 042702.
9. Bullough, C., Gatzen, C., Jakiel, C., Koller, M., Nowi, A., & Zunft, S. (2004). Advanced adiabatic compressed air energy storage for the integration of wind energy. In Proceedings of the European Wind Energy Conference (EWEC) Vol. 22, p. 25.

10. Li, Y., Wang, X., Li, D., & Ding, Y. (2012). A trigeneration system based on compressed air and thermal energy storage. *Applied Energy*, 99, 316-323.
11. Kim, Y. M. & Favrat, D. (2010) Energy and exergy analyses of a micro-compressed air energy storage and air cycle heating and cooling system. *Energy*, 35(1), 213-220.
12. Liu W, Liu L, Zhou L, Huang J, Zhang Y, Xu G, Yang Y. Analysis and optimization of a compressed air energy storage—combined cycle system. *Entropy*. 2014 :3103-20.
13. Zhao P, Wang J, Dai Y. Thermodynamic analysis of an integrated energy system based on compressed air energy storage (CAES) system and Kalina cycle. *Energy conversion and management*. 2015;98:161-72.
14. Budt, M., Wolf, D., Span, R., & Yan, J. (2016). A review on compressed air energy storage: Basic principles, past milestones, and recent developments. *Applied Energy*, 170, 250-268.
15. Wolf, D. & Budt, M. (2014). LTA-CAES—a low-temperature approach to adiabatic compressed air energy storage. *Applied Energy*, 125, 158-164.
16. Zhang, Y., Yang, K., Li, X., & Xu, J. (2013). The thermodynamic effect of thermal energy storage on compressed air energy storage system. *Renewable Energy*, 50, 227-235.
17. Xia, C., Zhou, Y., Zhou, S., Zhang, P., & Wang, F. (2015). A simplified and unified analytical solution for temperature and pressure variations in compressed air energy storage caverns. *Renewable Energy*, 74, 718-726.
18. Mozayeni, H., Negnevitsky, M., Wang, X., Cao, F., & Peng, X. (2017). Performance study of an advanced adiabatic compressed air energy storage system. *Energy Procedia*, 110, 71-6.
19. Luo, X., Wang, J., Krupke, C., Wang, Y., Sheng, Y., Li, J., Xu, Y., Wang, D., Miao, S., & Chen, H. (2016). Modelling study, efficiency analyses and optimization of large-scale Adiabatic Compressed Air Energy Storage systems with low-temperature thermal storage. *Applied Energy*, 162, 589-600.

20. He, Y., Chen, H., Xu, Y., & Deng, J. (2018). Compression performance optimization considering variable charge pressure in an adiabatic compressed air energy storage system. *Energy*, 165, 349-359.
21. Houssainy, S., Janbozorgi, M., & Kavehpour, P. (2018). Thermodynamic performance and cost optimization of a novel hybrid thermal-compressed air energy storage system actual. *Journal of Energy Storage*, 18, 206-217.
22. Kim, Y. M. (2012). Novel concepts of compressed air energy storage and thermo-electric energy storage. EPFL.
23. Mazloum, Y., Sayah, H., & Nemer, M. (2017). Dynamic modeling, and simulation of an isobaric adiabatic compressed air energy storage (IA-CAES) system. *Journal of Energy Storage*, 11, 178-190.
24. Bagdanavicius, A. & Jenkins, N. (2014). Exergy and exergo-economic analyses of a Compressed Air Energy Storage combined with a district energy system. *Energy Conversion and Management*, 77, 432-440.
25. Geissbühler, L., Becattini, V., Zanganeh, G., Zavattoni, S., Barbato, M., Haselbacher, A., & Steinfeld, A. (2018). Pilot-scale demonstration of advanced adiabatic compressed air energy storage, Part 1: Plant description and tests with sensible thermal-energy storage. *Journal of Energy Storage*, 17, 129-139.
26. Becattini, V., Geissbühler, L., Zanganeh, G., Haselbacher, A., & Steinfeld, A. (2018). Pilot-scale demonstration of advanced adiabatic compressed air energy storage, Part 2: Tests with combined sensible/latent thermal-energy storage. *Journal of Energy Storage*, 17, 140-152.
27. Ebrahimi, M., Carriveau, R., Ting, D. S., & McGillis, A. (2019). Conventional and advanced exergy analyses of a grid connected underwater compressed air energy storage facility. *Applied Energy*, 242, 1198-1208.
28. Carriveau, R., Ebrahimi, M., Ting, D. S., & McGillis, A. (2019). Transient thermodynamic modeling of an underwater compressed air energy storage plant: Conventional versus advanced exergy analyses. *Sustainable Energy Technologies and Assessments*, 31, 146-154.

29. Arabkoohsar, A., Dremark-Larsen, M., Lorentzen, R., & Andresen, G.B. (2017). Subcooled compressed air energy storage system for coproduction of heat, cooling, and electricity. *Applied Energy*, 205, 602-614.
30. Lv, S., He, W., Zhang, A., Li, G., Luo, B., & Liu, X. (2017). Modelling and analyses of a novel compressed air energy storage system for trigeneration based on electrical energy peak load shifting. *Energy Conversion and Management*, 135, 394-401.
31. Liu, J. L. & Wang, J.H. (2015). Thermodynamic analyses of a novel tri-generation system based on compressed air energy storage and pneumatic motor. *Energy*, 91, 420-429.
32. Han, Z. & Guo, S. (2018). Investigation of discharge characteristics of a tri-generative system based on advanced adiabatic compressed air energy storage. *Energy Conversion and Management*, 176, 110-122.
33. Li, Y., Wang, X., Li, D., & Ding, Y. (2012). A trigeneration system based on compressed air and thermal energy storage. *Applied Energy*, 99, 316-323.
34. Jannelli, E., Minutillo, M., Lavadera, A. L., & Falcucci, G. (2014). A small-scale CAES (compressed air energy storage) system for stand-alone renewable energy power plant for a radio base station: A sizing-actual methodology. *Energy*, 78, 313-322.
35. Venkataramani, G., Ramakrishnan, E., Sharma, M. R., Bhaskaran, A. H., Dash, P. K., Ramalingam, V., & Wang, J. (2018). Experimental investigation on small capacity compressed air energy storage towards efficient utilization of renewable sources. *Journal of Energy Storage*, 20, 364-370.
36. Cheayb, M., Gallego, M. M, Tazerout, M., & Poncet, S. (2019). Modelling and experimental validation of a small-scale trigenerative compressed air energy storage system. *Applied Energy*, 239, 1371-1384.
37. Bloch, H. P. (2006). *A Practical Guide to Compressor Technology*. John Wiley & Sons.
38. Shah, R. K. & Sekulic, D.P. (2003). *Fundamentals of Heat Exchanger Actual*. John Wiley & Sons.

39. Mohammadi, A. & Mehrpooya, M. (2017). Energy and exergy analyses of a combined desalination and CCHP system driven by geothermal energy. *Applied Thermal Engineering*, 116, 685-694.
40. Weib, A. P. Volumetric expander versus turbine—which is the better choice for small ORC plants. (2015). In 3rd International Seminar on ORC Power Systems, 12-14.
41. Wang, Z., Xiong, W., Ting, D. S., Carriveau, R., & Wang, Z. (2016). Conventional and advanced exergy analyses of an underwater compressed air energy storage system. *Applied Energy*, 180, 810-822.
42. Tsatsaronis G, Park MH. On avoidable and unavoidable exergy destructions and investment costs in thermal systems. *Energy conversion and management*. 2002 Jun 1;43(9-12):1259-70.

## VITA AUCTORIS

NAME: Raghuveera Sai Sarath Dittakavi

PLACE OF BIRTH: Andhra Pradesh, India

YEAR OF BIRTH: 1996

EDUCATION: V. R. Siddhartha Engineering College, B.  
Tech (Mechanical Engineering), Andhra  
Pradesh, India, 2018.